SEDIMENTOLOGY the journal of the International Association of Sedimentologists

Sedimentology (2021) **68**, 1797–1830 doi: 10.1111/sed.12849

STATE OF THE SCIENCE

Biogeochemical reappraisal of the freshwater–seawater mixing-zone diagenetic model

DANIEL A. PETRASH*,† , OR M. BIALIK‡,[1], PHILIP T. STAUDIGEL§, KURT O. KONHAUSER¶ and DAVID A. BUDD**

**Department of Environmental Geochemistry and Biogeochemistry, Czech Geological Survey, Geologická 6, Prague 152 00, Czech Republic (E-mail: daniel.petras@geology.cz)*

†SoWa Research Infrastructure, Biology Centre of the Czech Academy of Sciences, Branišovská 31, České Budějovice 370 05, Czech Republic

‡Department of Marine Geosciences, School of Marine Sciences, University of Haifa, Haifa 31905, Israel (E-mail: obialik@campus.haifa.ac.il)

§School of Earth and Ocean Sciences, Cardiff University, Cardiff CF10 3AT, UK

¶Department of Earth and Atmospheric Sciences, University of Alberta, Edmonton, AB T6G 2E3, Canada

***Department of Geological Sciences, University of Colorado, Boulder, CO, 80309, USA*

Associate Editor – Eric Hiatt

ABSTRACT

First proposed nearly half a century ago, the mixing-zone model of dolomitization enjoyed a brief stay in the limelight before falling out of favour. Despite extended past criticism, arguments that build on its current validity are presented and discussed. The coastal mixing zone can be seen as an aquifer system exhibiting marked physicochemical gradients, reflective of the admixture of low salinity freshwater and seawater sources with variable redox potentials. This perspective requires a more holistic look at the mixing zone, not only as a gradient of major element concentrations, but also as the locus of enhanced subsurface redox sensitive reactions that occur at the pore-space scale within a moveable diagenetic front. Combined genomic and isotopic data indicate that an active subsurface biosphere thrives in the mixing zone. This could facilitate Mg^{2+} dehydration, generate alkalinity, consume protons and mobilize potentially catalyzing ions (i.e. Mn and Zn), which are all low temperature factors thought to promote dolomite formation from soluble precursors. In the updated model, the advective mix of fluids with contrasting composition modulate a range of biogeochemically induced mineral dissolution and reprecipitation reactions. Biotic and abiotic interactions between these fluids affect carbonate equilibrium and result in dissolution of soluble aragonitic and calcitic phases, while dolomite precipitates (as cement) and neomorphic replacement. The secondary dolomite often exhibits compositional heterogeneity and contentious $\delta^{18}O$ signatures indicative of re-equilibration. The role of manganese, zinc, intermediate sulphur species and ammonia are far from being fully understood, nor is their fingerprint in ancient deposits. Application of *in situ* spectroscopic imaging techniques, clumped and metal isotope analyses, as well as a more extended use of traditional approaches, such as sulphur isotopes, are poised to open many opportunities to further explore the biogeochemistry of this diagenetic environment and how it relates to platform dolomitization.

[1]Present address: Department of Geosciences, Marine Geology & Seafloor Surveying, University of Malta, Msida, MSD 2080, Malta

Keywords Carbonate equilibria, Caribbean and west Gulf of Mexico, coastal aquifers, deep biosphere, diagenesis, groundwater hydrochemistry, Neogene platforms.

INTRODUCTION

The original mixing-zone dolomitization model involves the admixture of meteoric freshwater and seawater (Hanshaw *et al.*, 1971; Badiozamani, 1973; Land, 1973), and was widely used during the 1980s to explain the pervasive shallow burial dolomitization of subtidal marine carbonates not associated with evaporites (Choquette & Steinen, 1980; Gebelein *et al.*, 1980; Taberner & Santisteban, 1987; Xun & Fairchild, 1987; Coniglio *et al.*, 1988; Searl, 1988). The mixing-zone model was originally formulated based on the observed and calculated nonlinearity of carbonate mineral solubility regarding differences in ionic strength, total dissolved inorganic carbon (ΣCO_2), the partial pressure of carbon dioxide (pCO_2) and ionic activities in the endmember solutions. Such differences allow – under certain admixtures – for aragonite, and to a lesser extent calcite undersaturation (Plummer, 1975; Wigley & Plummer, 1976), with concomitant dolomite oversaturation (Fig. 1A). The thermodynamic instability of $CaCO_3$ polymorphs predicts that the partial dissolution and replacement of metastable skeletal grains and their preferential cementation by dolomite should be favoured in the mixing zones of unconfined and confined coastal aquifers (Folk & Land, 1975; Magaritz *et al.*, 1980).

By the end of the 1980s, the model began receiving strong criticism, notably by some of its former advocates, because of the conjecture that extreme oversaturation conditions are required for dolomite formation (Land, 1985, cf. Land, 1998). In addition, some authors noted that modern coastal mixing zones, as well as Pleistocene rocks that passed through multiple mixing zones due to glacioeustatic sea-level changes appear to be largely devoid of dolomite (e.g. Machel & Mountjoy, 1986). Those observations, in turn, were used to argue that mixing zones did not produce dolomite as the model predicted. In addition, the recognition of extensive dissolution in modern and Upper Neogene platformal successions (e.g. Back *et al.*, 1986; Mylroie & Carew, 1990) promoted the notion that the main diagenetic process in mixing zones is dissolution, not precipitation. The mixing-zone dolomitization model was further weakened when Land (1991) rebutted his earlier (Land, 1973) application of the model to the Plio-Pleistocene Hope Gate Formation of Jamaica. Subsequently, the role of freshwater–-seawater admixture in diagenesis was relegated only to generation of calcite (Muchez & Viaene, 1994; Vahrenkamp & Swart, 1994), with more recent reaction transport modelling even suggesting that such a circulation regime could produce only small amounts of dolomite, if any, due to slow fluid fluxes (Xiao *et al.*, 2013). By the mid-2000s, the mixing-zone dolomitization model was called into question and refuted (Machel, 2004; Melim *et al.* 2004).

However, these lines of argument against the mixing-zone model conflict with compelling field evidence that does suggest dolomite formation within some modern mixing zones. For example, Matsuda *et al.* (1995) and Stüben *et al.* (1996) noted Mg depletion and Ca enrichment in dolomite supersaturated mixtures of freshwater –seawater. In both cases, dolomitization was inferred, and Stüben *et al.* (1996) supported their inference with documentation of authigenic dolomite in the associated cave walls and cave sediments. Whitaker & Smart (1998) noted that mixing-zone waters in a blue hole on the east coast of South Andros Island, Bahamas, approached equilibrium with respect to disordered dolomite and that bulk rock analyses of wall rocks in the modern mixing zone had measurable enrichments in magnesium relative to wall rocks above and below the mixing zone. Whitaker & Smart (1998) suggested that those observations might indicate localized dolomitization, influenced by organic matter oxidation coupled to both iron and sulphate respiration (see also Smart *et al.*, 1988). Onac *et al.* (2014) demonstrated the presence of authigenic dolomite at the bedrock/brackish water interface in speleothem deposits of Cova des Pas de Vallgornera, Mallorca, Spain. These, and other similar observations (Shatkay & Magaritz, 1987; Sumrall *et al.*, 2015), require a re-examination of the mixing-zone dolomitization model with modern, unbiased and holistic eyes.

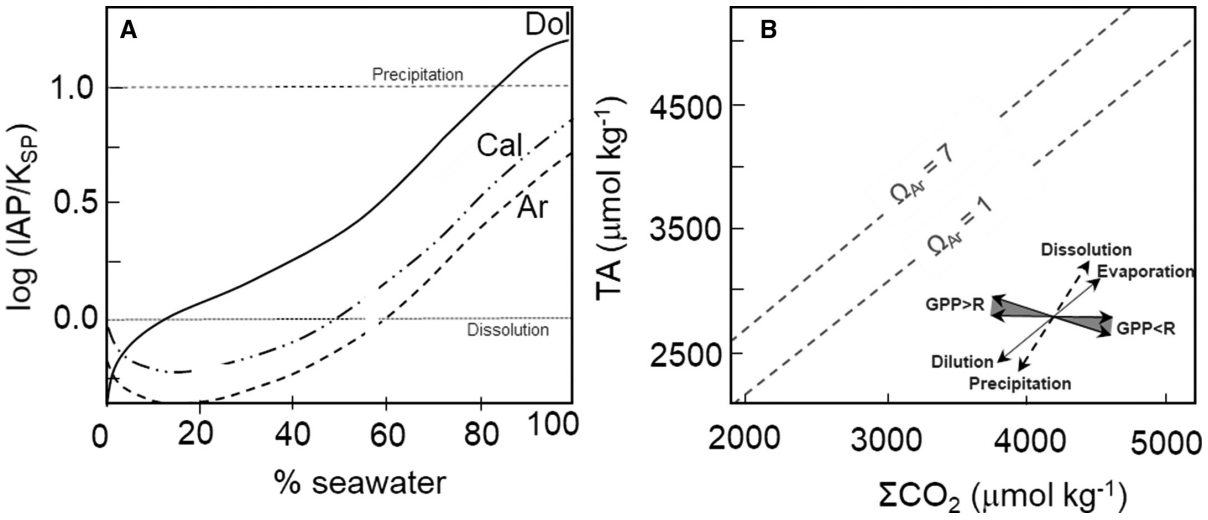

Fig. 1. The dynamics of the seawater CO_2-carbonic acid system in the mixing zone. (A) An early conception comparing the saturation index (log (IAP/K_{SP}) of dolomite, calcite and aragonite as function of salinity (modified from Herman *et al.*, 1985). Calculations used Caribbean seawater and Yucatan freshwater as end members of conservative mixing. The mixing of marine and meteoric waters results in a decrease in the Mg/Ca ratio of the diagenetic fluid, which is generally thought to decrease the saturation state of dolomite. (B) Under constant temperature and salinity, the ΣCO_2 to total alkalinity (TA) ratio controls the speciation of dissolved inorganic carbon and carbonate mineral saturation states (Ω). For the case of aragonite, if ΣCO_2 and TA change in a ratio of 1.05, there will be no net change in groundwater Ω. If they change to a ratio >1.05, aragonite Ω increases, and if the relation is <1.05, that Ω decreases. Hydrochemical analyses show that in mixing-zone examples evaluated here, the ΣCO_2 to TA ratio ranges from 0.96 to 1.08 (Table 1). Consequently, the admixture of freshwater and seawater (or partially evaporated seawater) and subsurface biogeochemical processes [chemoautotrophy (GPP) versus heterotrophy (*R*)], with their contrasting effects over the mixed freshwater–groundwater ΣCO_2 to TA ratio, exert a key control over dissolved inorganic carbon speciation, pH and dissolution/precipitation processes (inset).

Refinements that can now revive the mixing-zone dolomitization model in a new form after being refuted as originally stated, include growing insights into carbonate speciation, microbial activity and electron transfer mechanisms in mixing zones. For instance, the dynamics of carbonate species in coastal groundwaters are now recognized as being much more complex and variable than previously thought (Soetaert *et al.*, 2007; Dickson, 2010; Hagens & Middelburg, 2016). As shown in Table 1, if the change of ΣCO_2 and total alkalinity (TA) remains in a ratio of *ca* 1.05 during mixing, there is no net change in the saturation state of aragonite (Ω_{Ar}; Fig. 1B; Mackenzie & Andersson, 2013). In addition, processes such as transport of organic matter (OM) or its production by chemoautotrophs (i.e. microorganisms that produce organic carbon from dissolved CO_2 without the involvement of light) and the accompanying heterotrophic activity are now thought as crucial agents in the carbonate system (Middelburg, 2019; Fig. 1B).

The mixing of endmember fluids can also effectively drive the local availability of electron donors and acceptors that enhance certain subsurface microbial functions. Hence, microbial activity in coastal aquifers may be capable of inducing dolomite precipitation by sustaining elevated pH and porewater alkalinity and/or by promoting Mg^{2+} cation dehydration within biofilms (Petrash *et al.*, 2017). A revised freshwater–seawater mixing-zone model thus envisions a dynamic diagenetic front that results in the enhanced activity of subsurface microbes (Petrash *et al.*, 2017). Microbial activity in such biogeochemically reactive interfaces, notably with respect to transitional metal reduction and recycling, induces the stabilization of partially ordered Ca-dolomite from metastable precursors such as very high-Mg calcite (VHMC; i.e. >30 mol.% $MgCO_3$), with the former poised to recrystallize to more ordered dolomite through solid state reorganization (for example, Ostwald ripening). Recrystallization most probably

Table 1. Hydrochemical parameters of the modern mixing zone in the Cenozoic platforms considered herein.

Location	Ca^{2+} (mM)	Mg^{2+} (mM)	Sr^{2+} (μM)	Fe^{2+} (nmol kg^{-1})	Mn^{2+} (nmol kg^{-1})	SO_4^{2-} (mM)	Salinity (psu)	$\delta^{13}C$ $(‰)_{V\text{-}PDB}$	$\delta^{18}O$ $(‰)_{SMOW}$	DOC (μM)	pH	TA (μmol kg^{-1})	ΣCO_2 (μmol kg^{-1})	ΣCO_2/TA
Central Florida Suwannee Formation (Sacks & Tihansky, 1996)	3 to 11	3 to 21	168 to 643	180 to 3580	46*	4 to 19	1 to 15	−6.5 to −5.8	−1.9 to −1.0	125 to 183	7.0 to 7.3	3044	2971 to 3357	0.97 to 1.10
Central Florida Base Ocala/Top Avon (Cander, 1992; Katz, 1992; Sacks & Tihansky, 1996)	9 to 8	3 to 6	273 to 285†	180 to 1074	182 to 1092	1 to 8	1 to 14	−5.7 to −3.5	−4.1 to −1.2	8.3 to 316	7.6	1723 to 2805	1775 to 2935	0.96 to 1.03
Curaçao and Bonaire (Fouke, 1993; van Sambeek *et al.*, 2000)	3 to 19	3 to 27	n.d.	n.d.	n.d.	1 to 3	1 to 30		−4.0 to −2.0		7.2 to 7.5	4562 to 7487	4671 to 8077	1.01 to 1.08
Yucatan SE (Socki *et al.*, 2002; Frausto *et al.*, 2008; Gondwe *et al.*, 2010; Gonneea *et al.*, 2014; Brankovits *et al.*, 2017)	4 to 20	6 to 9	1 to 60‡	322 to 13180	18 to 3349	14 to 19	1 to 37	−10.4 to −11.8	−5.3 to −2.1§	105 to 147	6.8 to 8.6	5788 to 7456¶	6245 to 7904¶	1.04 to 1.08

*Value is a half of the reported DL. †Sacks (1996) reports local [Sr] as high as 94 mM linked – dissolution of celestite. ‡Socki *et al.* (2002) reports significant $[Sr^{2+}]$ and $[SO_4^{2-}]$ correlation linked to dissolution of celestite. §Stoessell *et al.* (1989) report less negative to neutral values. ¶In the reducing brackish water of a cenote, Gonneea *et al.* (2014) reports TA as high as 13644 μmol kg^{-1} (ΣCO_2 = 14359 μmol kg^{-1}; pH 6.8).

occurs throughout discrete microscale dissolution–reprecipitation stages (Nordeng & Sibley, 1994; Kaczmarek & Sibley, 2014). Repeated establishment of such biogeochemically reactive interfaces through time over a package of carbonate rocks can result in the dolomite being stratigraphically well distributed. This dolomite could form as neomorphic replacement of precursor carbonates or cements in open void spaces ranging from the submicron scale (i.e. between micritic crystals) to intergranular pores and the walls of larger macroscopic dissolution vugs (mixing-zone 'sponge rock' *sensu* Back *et al.*, 1986; or flank-margin cavernous, *sensu* Mylroie & Carew, 1990).

In this work, the biogeochemistry of freshwater–seawater mixing zones is evaluated in terms of hydrochemistry and microbial community structure. A revised diagenetic model of the mixing zone with an emphasis on its potential to be a zone of dolomite formation is then presented. Some proposed examples of Cenozoic mixing-zone dolomites from around the Gulf of Mexico and the Caribbean provide further details of potential textures, luminescence, isotopic and trace element signatures of mixing-zone dolomites. These examples include the Eocene–-Oligocene of the Central Florida Platform, the Mio-Pleistocene of Bonaire and Curaçao, Holocene of north-eastern Yucatan Platform, Isla de Monas in Puerto Rico, South Andros Island in the Bahamas and Ambergris Cay in Belize (Ward & Halley, 1985; Mazzullo *et al.*, 1987; Cander, 1994; Fouke *et al.*, 1996; González *et al.*, 1997; Whitaker & Smart, 1998; Teal *et al.*, 2000; Gaswirth *et al.*, 2007; Sumrall *et al.*, 2015). Finally, from the comparative analysis of the textural, chemical and isotopic variabilities of the dolomite locales re-evaluated here, this work emphasizes the need for systematic facies-scale to crystal-scale studies of the geochemical and potentially isotopic composition of possible ancient mixing zones. The cementing phases formed therein are potential windows for understanding the long term-dynamics, kinetics and bioenergetics of subsurface life, and the crucial role of the latter in differential diagenesis and rock-selective dolomitization.

Microbial involvement in shallow burial dolomite formation

The interaction between biochemical and hydraulic gradients in the mixing zone forms an environment with a wide range of pH, redox potential (Eh), alkalinity, ionic strength and ionic speciation that can favour microbial catalysis of dolomite. The more traditional interpretation (Dorag model, *sensu* Badiozamani, 1973) would limit these effects only to the modification of relative saturation state of calcite and aragonite versus that of dolomite (Smart *et al.*, 1988). However, the dolomite precipitation rate is not linear with respect to saturation state, and every two-fold increase in the saturation state of dolomite results in a five-fold to nine-fold increase in precipitation rate (Arvidson & Mackenzie, 1997). As a result of that non-linearity, the dolomite precipitation rate will still not be as fast as the calcite precipitation rate (Zuddas & Mucci, 1994).

In the past three decades, studies of synthetic dolomite precipitated under the influence of prokaryotes isolated from hypersaline settings have demonstrated that microbial activity is involved in formation of dolomite (Vasconcelos *et al.*, 1995; Warthmann *et al.*, 2000; Wright & Wacey, 2005), or its VHMC precursors (Gregg *et al.*, 2015). Subsequent laboratory experiments and numerous empirical observations in modern dolomite forming settings reinforced the notion that some microbial metabolic pathways could play an important role in the formation of dolomite (Petrash *et al.*, 2017). In the most general sense, anaerobic heterotrophy (for example, the reduction of manganese, iron and sulphate) all generate localized alkalinity, while sulphate reduction also plays a role in liberating Mg^{2+} from the soluble aqueous $MgSO_4$ complex. Whether dolomite formation is a direct product of microbial metabolic activity or is rather mediated by the reactivity of microbial exopolymers (EPS) toward Ca^{2+} and Mg^{2+} ions remains an ongoing debate. In addition, more recent experiments have demonstrated that an increase in mobile transition metals such as Mn and Zn have a catalyzing function (Daye *et al.*, 2019; Vandeginste *et al.*, 2019) that other studies have ascribed to dissolved sulphide and the exopolymers excreted by microbes (Zhang *et al.*, 2012a; Roberts *et al.*, 2013).

In recent years the microbial model for dolomite formation has generated significant debate, both with supporters and detractors (Gregg *et al.*, 2015; Petrash *et al.*, 2017; Manche & Kaczmarek, 2019). Kinetic studies (Kell-Duivestein *et al.*, 2019) have demonstrated that activation energy for the transition to fully crystalline dolomite is much lower for a disordered near-stochiometric precursor than a non-stochiometric

precursor. Extrapolation of results from high temperature experiments to lower temperature diagenetic realms indicate that the time needed for these products to achieve a poorly ordered dolomite could be under a year at 25°C but may take up to 6.8 Myr to become near-stoichiometric dolomite (Kell-Duivestein *et al.*, 2019). These findings reinforce empirical results where synthetic Ca-rich microbial dolomite often shows poorly expressed reflections (i.e. {101}, {015}, {021}), indicative of poor lattice order (Gregg *et al.*, 2015). These properties also characterize some Late Neogene dolomite deposits (e.g. Van Lith *et al.*, 2003), which supports the viability of syngenetic microbial precipitates as the poorly ordered precursor that must go through ripening and aging for shallow burial diagenetic dolomite formation in the larger scale geological context. In such a context, the diagenetic imprint of most Neogene carbonate platforms records a significant chapter attributed to the mixing of freshwater and seawater. The biogeochemical conditions under which mixing-zone diagenesis occurs affect the dynamics of elemental cycles relevant to the carbonate system, with subsurface prokaryote communities defining redox budgets and transformations that could influence dolomitization at different temporal and spatial scales.

BIOGEOCHEMICAL TRANSFORMATIONS IN THE MIXING ZONE

The spatial distribution and temporal evolution of microbial functions capable of driving rate-limiting diagenetic processes, such as organic carbon turnover, are yet to be fully investigated in extended coastal aquifers such as those considered here. Despite the limitation imposed for the lack of systematic studies characterizing the subsurface biosphere functioning in Cenozoic carbonate platforms, this section considers and relates diverse data from discrete coastal mixing zones to offer a general perspective on the biogeochemical conditions relevant to CO_2 equilibria in the coastal mixing zone.

Table 1 illustrates the variability observed in key parameters of modern mixing zones that occur primarily in Neogene limestone rock units that also contain substantial dolomite-bearing successions. This variability suggests that steep redox gradients can form within the mixing zone (Fig. 2) in association with discrete metabolic reactions (Table 2). The multistep or cascade reactions governing these transformations regulate parameters such as ΣCO_2, alkalinity and pH buffering. Coupled with the effects of temperature and salinity (Mucci, 1983; Lee & Millero,

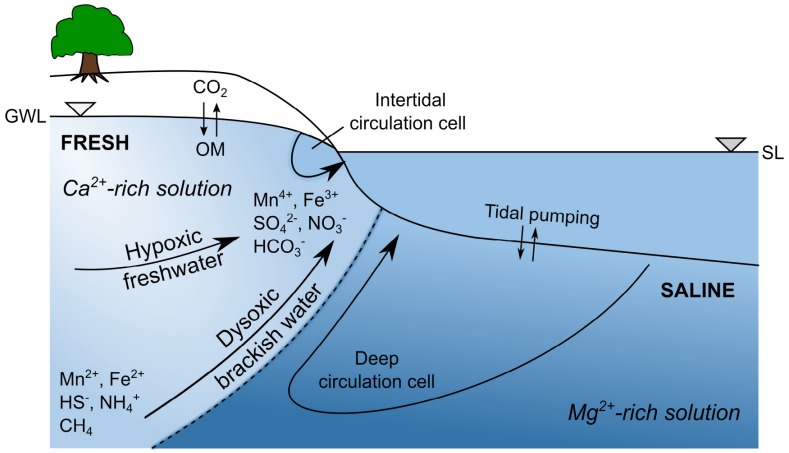

Fig. 2. A simplified scheme of an unconfined coastal aquifer system with deeper sourced fluxes of bioactive chemical species (for example, Yucatan, Central Florida). Groundwater level and flow is controlled by seasonal climate and inland hydraulic gradients. Relative sea-level changes can affect tides and circulation cells flows. An active transformation of electron donors/acceptors occurs across this coastal aquifer system and, consequently, redox gradients develop and exert critical controls over carbon turnover (OM ⇋ CO_2 ⇋ CH_4). Other reactants (for example, seawater-derived Mg^{2+}) are delivered to the active sites of carbonate precipitation by circulation cells driven by salinity gradients.

Table 2. Metabolic reactions involving organic matter (OM) respiration and predicted effects on carbon equilibrium conditions (after Soetaert *et al.*, 2007 and Loyd *et al.*, 2012).

		dpH	ΔTA*	ΔΣCO_2	ΔTA/ ΔΣCO_2
Aerobic oxidation					
(1)	$(CH_2O)_{106}(NH_3)_{16}H_3PO_4 + 138O_2 + 16HCO_3^- \rightarrow 16NO_3^- + 0.5HPO_4^{2-} + 0.5H_2PO_4^- + 122CO_2 + 138H_2O + 1.5H^+$	-1.32×10^{-3}	–17.5	+106	–0.17
Nitrate reduction					
(2)	$(CH_2O)_{106}(NH_3)_{16}H_3PO_4 + 94.4NO_3^- + 92.9H^+ \rightarrow 55.2N_2 + 0.5HPO_4^{2-} + 0.5H_2PO_4^- + 106CO_2 + 177.2H_2O$	-0.26×10^{-3}	+93.4	+106	+0.88
(3)	$NO_3^- + HS^- + H_2O + H^+ \rightarrow NH_4^+ + SO_4^{2-}$		+1		
Manganese reduction					
(4)	$(CH_2O)_{106}(NH_3)_{16}H_3PO_4 + 212MnO_{2(s)} + 318CO_2 + 106H_2O + 13.5H^+ \rightarrow 15NH_4^+ + 0.5HPO_4^{2-} + 0.5H_2PO_4^- + 424HCO_3^- + 212Mn^{2+}$	$+3.94 \times 10^{-3}$	+438	+106	+4.13
Iron reduction					
(5)	$(CH_2O)_{106}(NH_3)_{16}H_3PO_4 + 424Fe(OH)_{3(s)} + 742CO_2 + 13.5H^+ \rightarrow 15NH_4^+ + 0.5HPO_4^{2-} + 0.5H_2PO_4^- + 848HCO_3^- + 424Fe^{2+} + 318H_2O$	$+9.2 \times 10^{-3}$	+862	+106	+8.13
Sulphate reduction					
(6)	$(CH_2O)_{106}(NH_3)_{16}H_3PO_4 + 53SO_4^{2-} + 13.5H^+ \rightarrow 15NH_4^+ + 0.5HPO_4^{2-} + 0.5H_2PO_4^- + 53CO_2 + 53HCO_3^- + 53HS^- + 53H_2O$	-0.64×10^{-3}	+67	+106	+0.63
Methanogenesis					
(7)	a) $(CH_2O)_{106}(NH_3)_{16}H_3PO_4 \rightarrow 0.5CO_2 + 16NH_3 + H_3PO_4 + 0.5CH_4$	-0.58×10^{-3}	+15	−1	0
	b) $2HCO_3^- + 4H_2 \rightarrow CH_4 + CO_3^{2-} + 3H_2O$		0	−1	0
Anaerobic oxidation of methane					
(8)	(a) $CH_4 + 4MnO_2 + 7H^+ \rightarrow HCO_3^- + 4Mn^{2+} + 5H_2O$ (b) $CH_4 + 8Fe(OH)_3 + 15H^+ \rightarrow HCO_3^- + 8Fe^{2+} + 21H_2O$ (c) $CH_4 + SO_4^{2-} \rightarrow HCO_3^- + HS^- + H_2O$	-0.13×10^{-3}	+1	+1	+1

*$TA \approx 2(CO_3^{2-}) + HCO_3^- + OH^- + HPO_4^{2-} - H^+$.

1995; Millero, 1995), those parameters ultimately control carbonate precipitation and/or dissolution. In the case of the latter, hydrochemical mixing, CO_2 generated by oxidation of organic matter, or H^+ formed by re-oxidation of reduced sulphur species are well established aragonite and Mg-calcites' dissolution/reprecipitation agents in upper mixing zones (Bottrell *et al.*, 1991; Stoessell, 1992; Whitaker & Smart, 1998). However, precipitation of dolomite linked to biogeochemical transformations was not considered in either the initial conceptualization of the mixing-zone model or in subsequent criticisms of the original conception. When a favourable set of reactions consuming protons and producing alkalinity occur at any point in time, they should promote the formation of a spatially restricted body of carbonate mineralization, including dolomite. To understand how these reactions impact dolomitization, it is necessary to consider the distribution, availability and likely modes of utilization of microbial energy sources in the mixing zone.

Bioenergetics in the mixing zone: temporal and spatial variability

This section considers the general distribution and transformations of terminal electron acceptors (TEA) and organic matter stocks reported in discrete confined and unconfined coastal aquifer examples featuring Neogene dolomite successions. This study also causally connects such transformations with concurrent changes in carbonate equilibrium and other relevant hydrochemical variables also reported, including, for instance, S and C isotope proxies. Together the data available point to an active recycling of bioactive elements within modern coastal mixing zones.

In addition to the vertical zonation of electron acceptors/donors typically observed in marine

sediments (Froelich *et al.*, 1979; Konhauser, 2007), biogeochemical processes in coastal groundwaters can lead to complex patterns in the distribution and speciation of nitrogen, sulphur, manganese and iron along the axis of the hydraulic gradient (Lovley & Chapelle, 1995). Due to this biogeochemical complexity, carbonate equilibrium in the mixing zone can be locally impacted by the segregated distribution and activity rates of micro-organisms capable of driving carbon turnover and alkalinity production throughout the cycling of bioactive elements.

Many reviews exist on the role of biogeochemistry in carbonate systems (Zeebe & Wolf-Gladrow, 2001; Soetaert *et al.*, 2007; Wolf-Gladrow *et al.*, 2007; Middelburg, 2019). In the continuum of organic matter degradation processes (Boudreau & Ruddick, 1991; Beulig *et al.*, 2018), these reactions (Table 2) are the energy source sustaining long-term microbial functioning.

The distribution of biogeochemical zones within modern unconfined coastal mixing zones has been studied via localized electrochemical measurements and chemical analyses (Charette & Sholkovitz, 2002; Kroeger & Charette, 2008; Rodellas *et al.*, 2015). Nonetheless, in timescales of 10^5 to 10^6 years, the location and geometry of redox gradients within confined and unconfined systems can be strongly modified by changes in relative sea level and climate, with the latter acting as a dynamical system that has a non-linear response to quasi-periodic orbital forcing (Westerhold *et al.*, 2020). The zone of maximum redox gradient (i.e. the redoxcline) in unconfined coastal mixing zones can also change fortnightly due to tides (Taniguchi, 2002; Boehm *et al.*, 2006; De Sieyes *et al.*, 2008), and seasonally due variations in recharge (Michael *et al.*, 2005; Charette, 2007), both of which also affect the location and depth of the halocline (i.e. the zone of maximum salinity gradient). In addition, multiple geological, hydrological and hydraulic variables affect groundwater flow paths and mixing through the heterogeneous subsurface features of coastal landmasses resulting in a patchwork-like pattern of diagenetic effects across large-scale hydrogeological systems (Chapelle *et al.*, 1995; Befus *et al.*, 2017).

Oxygen availability, organic matter turnover and ΣCO_2

Dissolved oxygen (DO) can be introduced into the aquifer via recharge, thus facilitating aerobic oxidation of dissolved organic matter, or DOM (Table 2, Reaction 1). This DOM is comprised of organic acids, humic substances, polysaccharides, short chain hydrocarbons and other biomolecules. Groundwater can then remain partially oxygenated where there is a general lack of DOM and other electron donors, such as reduced sulphur species that support microbial O_2 reduction (McMahon, 2001). The redox chemistry of fresh and mixing-zone waters could be expressed in terms of the flow path. Models of the confined Intermediate and Upper Floridan aquifers show that downdip of the coastal mixing zone, and along the axis of the hydraulic gradient, there is significant variation in DO linked to terrestrial DOM inputs (Sacks & Tihansky, 1996). Similarly, the halocline in the unconfined Yucatan aquifer has been recently portrayed as a 'conveyor belt' for the transport of terrestrial DOM from hypoxic to anoxic zones (Calderón-Gutiérrez *et al.*, 2018). In the anoxic mixing zone of Yucatan, the involvement of methanogenic archaea was also assumed to contribute to the DOM supply because these chemoautotrophs produce abundant organic carbon (Pohlman *et al.*, 1997; Brankovits *et al.*, 2017).

In the modern mixing zone of the Upper Floridan Aquifer, the measured variability in ΣCO_2 ranges from 1400 to 3500 μatm (Table 1). The groundwater ΣCO_2 is significantly correlated with DOM and, to a lesser extent, the concentrations of reduced S species (Katz, 1992; Sacks & Tihansky, 1996). Brankovits *et al.* (2017) observed similar covariation of ΣCO_2 and DOM in the mixing zone of Yucatan. The redox environment of the modern mixing zone on Curaçao and Bonaire remains to be investigated, but Fouke (1993) noted that unpublished groundwater monitoring data from Curaçao record bicarbonate (HCO_3^-) concentrations ranging between 197 ppm and 488 ppm that increased toward hypoxic zones. In Curaçao, Fouke *et al.* (1996) also reported Ca-dolomite oversaturation in the groundwater system from a combination of basalt dissolution, which supplied dissolved Ca, Mg, Sr ions and anaerobic respiration of DOM generating HCO_3^- and additional alkalinity.

In near shore groundwaters another mechanism that modulates dissolved species is ebb tidal pumping of seawater into the coastal aquifer (Santos *et al.*, 2009a,b). In the east coast of South Andros Island, Bahamas, Whitaker & Smart (1998) reported that this mechanism caused enhanced mixing within fracture-related

caves. A freshwater lens underlying the island gives way to a brackish lens in the vicinity of the fracture system. The salinity of the brackish lens increases with depth and their waters are geochemically distinct from those of the surrounding freshwater lens because of inputs of surface-derived DOM. Carbonate supersaturation at shallow depths in both fresh and brackish waters results from degassing of CO_2 sourced from organic matter (OM) oxidation. Below this shallow zone, waters exhibit variable equilibrium conditions with regard to carbonate minerals (Whitaker & Smart, 1998).

Nitrogen

Biogeochemical and numerical studies conducted on modern mixing zones show that an availability of labile DOM rapidly exhausts DO and dissolved nitrate (NO_3^-) levels (Table 2, Reaction 2), while enriching the porewater in ammonia (NH_4^+; Table 2, Reaction 3; Santoro, 2010) and bicarbonate, which increases alkalinity and pH. However, the distribution of NO_3^-- and NH_4^+ across coastal aquifers has been found to exhibit complex temporal patterns (Santos *et al.*, 2008, 2012). For instance, there are zones where NO_3^- and NH_4^+ seem to co-exist in measurable quantities, suggesting the existence of a diverse microbial community. That community would be capable of combining heterotrophic and chemoautotrophic processes, for instance coupling either ammonium oxidation to Mn(IV) reduction (Reaction R1) or Mn(II) oxidation to nitrate reduction (Reaction R2) (Sørensen, 1987; Hulth *et al.*, 1999; Kroeger & Charette, 2008; Santoro, 2010).

$$NH_4^+ + 4MnO_2 + 6H^+ \rightarrow 4Mn^{2+} + NO_3^- + 5H_2O \quad \text{(R1)}$$

$$5Mn^{2+} + 2NO_3^- + 4H_2O \rightarrow 5MnO_2 + N_2 + 8H^+ \quad \text{(R2)}$$

Although some of these metabolisms are chemolithotrophic, and thus do not directly involve formation of bicarbonate, they can significantly impact pH and pCO_2 through CO_2 fixation to organic carbon (Thorstenson & Mackenzie, 1974; see also Middelburg, 2019) and may ultimately facilitate dolomite formation (Slaughter & Hill, 1991).

Transition metals

Mobility of redox sensitive trace metals in porewaters is governed by the redox potential (Eh) and pH of the pore fluid, with some transitional metals being immobilized by their co-precipitation with Mg and Ca into carbonates (notably Fe and Mn), or forming oxyhydroxide or sulphide solid phases. Therefore, Eh variability in the mixing zone does not only affect the precipitation/dissolution rates of carbonates, but also those of other coexisting mineral phases. Cyclic interaction with DO within coastal mixing zones can result in re-oxidation, mobilization, and changes in affinity and binding properties of transition metals. Therefore, DO exhaustion in mixing-zone diagenetic realms is usually accompanied by measurable changes in the stratigraphic distribution (partitioning) or redox sensitive elements. Moreover, the bioutilization of these metals is at times linked to that of other TEA that might also be available. For instance, several lines of recent metagenomic evidence show that subsurface communities that actively metabolize nitrate also impact the interlinked Fe and S cycles, (for example, Reactions R3 and R4) (Jewell *et al.*, 2016, 2017; Starke *et al.*, 2017).

$$10Fe^{2+} + 2NO_3^- + 24H_2O \rightarrow 10Fe(OH)_3 + N_2 + 18H^+ \quad \text{(R3)}$$

$$5HS^- + 8NO_3^- \rightarrow 5SO_4^{2-} + 4N_2 + 3OH^- + H_2O \quad \text{(R4)}$$

Portions of modern mixing zones are now known to host a reactive area in which fresh anoxic groundwaters provide Fe(II) that is locally oxidized and stabilized as ferric oxyhydroxide phases [for example, $Fe(OH)_3$; FeOOH] upon mixing with the brackish hypoxic groundwater (Charette & Sholkovitz, 2002; Johannesson *et al.*, 2011; McAllister *et al.*, 2015). These ferric oxyhydroxides can later serve as a substrate for Fe(III)-reduction once DO is exhausted. Continued transition down the TEA ladder will further decrease Eh to establish increasingly reducing conditions. Then Mn(IV, III) and Fe(III) are progressively used prior to the unset of dissimilatory sulphate reduction. However, re-establishment of DO in a previously anoxic part of the mixing zone can re-oxidize the Fe(II) and Mn(II) stocks.

In the fractured cave system encompassing the modern mixing zone on the east coast of South Andros Island, microbial processes involving Fe-oxidation were found to be responsible for dissolution of calcite and aragonite, while the lower mixing-zone waters remained saturated

with respect to dolomite (Whitaker & Smart, 1998). For example, maximum $CaCO_3$ dissolution was found to occur in the freshwater phreatic zone where ferric oxyhydroxides can be found coating the cave wall. As shown in Reaction R3 above, denitrification coupled to Fe(II) oxidation significantly impact the pH of ambient water. Whitaker & Smart (1998), however, attributed the additional dissolution potential in the upper mixing zone to an increase in ΣCO_2 linked to the microbial oxidation of OM coupled to dissimilatory Fe(III) reduction (Table 2, Reaction 5).

Excess CO_2 in the groundwater is degassed at the water table, progressively lowering pCO_2 just toward the lower mixing zone. Although dolomite was not apparent in thin sections of the Bahamian cave system, elemental analysis of the wall rock revealed bulk Mg enrichments in the modern mixing zone as compared with wall rocks located at the saline and freshwater end members (Whitaker & Smart, 1998). Recent dolomite found in submarine sinkholes at far field interaction between seawater and freshwater at the Great Bahama Bank exhibits Fe and Mn enrichment attributed to reductive conditions (Whitaker *et al.*, 1994). Similarly, Gebelein *et al.* (1980) documented patchy disordered dolomite formation only in tidal flat facies intersected by the modern freshwater–seawater mixing zone.

Interestingly, in the subsurface of the Abu Dhabi sabkha, Chafetz & Rush (1994) documented sabkha-type Pleistocene dolomite with nearly ideal stochiometric composition that contrasts with that formed since the Quaternary under evaporitic conditions. Stable oxygen isotope and elemental concentration analyses of those Pleistocene sabkha sequences suggests that the diagenetic fluid responsible for dissolution of precursory phases and cementation by dolomite likely includes relevant proportions of a meteoric endmember. Dolomitization also appears to have occurred more intensively in facies exhibiting Mn enrichments (Chafetz *et al.*, 1999). Similarly, in the Little Bahama Bank, Vahrenkamp & Swart (1994) reported on marked Mn and Fe enrichments in Mio-Pliocene dolomite crusts. These crusts predominantly formed under marine phreatic conditions but were also influenced by a palaeo-mixing zone. Also, in the modern mixing zone of Curaçao, van Sambeek *et al.* (2000) reported that the presence of more alkaline, dolomite saturated brackish groundwaters coincides with a step concentration gradient of dissolved Fe(II).

Different lines of evidence have more recently pointed to dissolved Mn and Zn as potentially important catalyzers of early diagenetic ordered dolomite nucleation (Daye *et al.*, 2019; Li *et al.*, 2019a; Vandeginste *et al.*, 2019). In fresh coastal aquifers, dissolved Mn concentrations are generally <100 nmol kg^{-1} but are often comparatively enriched in the higher salinity reducing groundwaters (Table 1). Moreover, Mn(IV) reduction coupled to organic matter oxidation (Table 2, Reaction 4) is the second most powerful alkalinity generator (Fig. 3). Mn(II) availability in sulphate/carbonate-bearing aqueous media are highly dependent on the redox state of the solution, and under high pH, low Eh regimes it becomes incorporated into carbonate minerals (Ham, 1972; Barnaby & Rimstidt, 1989; Li *et al.*, 2019b). A mechanism of continuous alkalinity generation might, in turn, be related to biological recycling of Mn in the presence of S^0 (Petrash *et al.*, 2015). Zinc concentrations in uncontaminated parts of the Florida aquifer are usually around 2 to 12 nmol kg^{-1}, although an increase occurs downgradient where waters from deeper in the confined aquifer are upwelling toward the discharge zone along the modern shoreline (Tang & Johannesson, 2005). In the Mio-Pleistocene of Bonaire aquifer Zn (and Sr) enrichment is observed in dolomite cements. These elements are thought to be sourced from the interaction of mixed source water with the meteorically altered basaltic basement (Fouke *et al.*, 1996). Zinc availability is affected by pH and the presence of sulphides which precipitate any available Zn (Krężel & Maret, 2016). As such, the optimal range for the presence of both of these ions (Mn^{+2} and Zn^{+2}), and their possible catalyzing effect over dolomitization, would be in a reduced, but not sulphidic, medium at pH of 7 to 8 and Eh in the range −100 to −200 mV. Such conditions are reported, for instance, in the coastal unconfined Upper Florida aquifer (Haque & Johannesson, 2006).

Sulphur respiration and methane production/oxidation

Sulphate reduction (Table 2, Reaction 6) and methanogenesis (Table 2, Reactions 7a and 7b) are the terminal metabolic pathways involved in changes in ΣCO_2 and DOM concentrations, and both reactions are thought to exert some control over the diagenetic conditions of dolomite formation (Petrash *et al.*, 2017). Sulphate reduction has been found to be an important process in

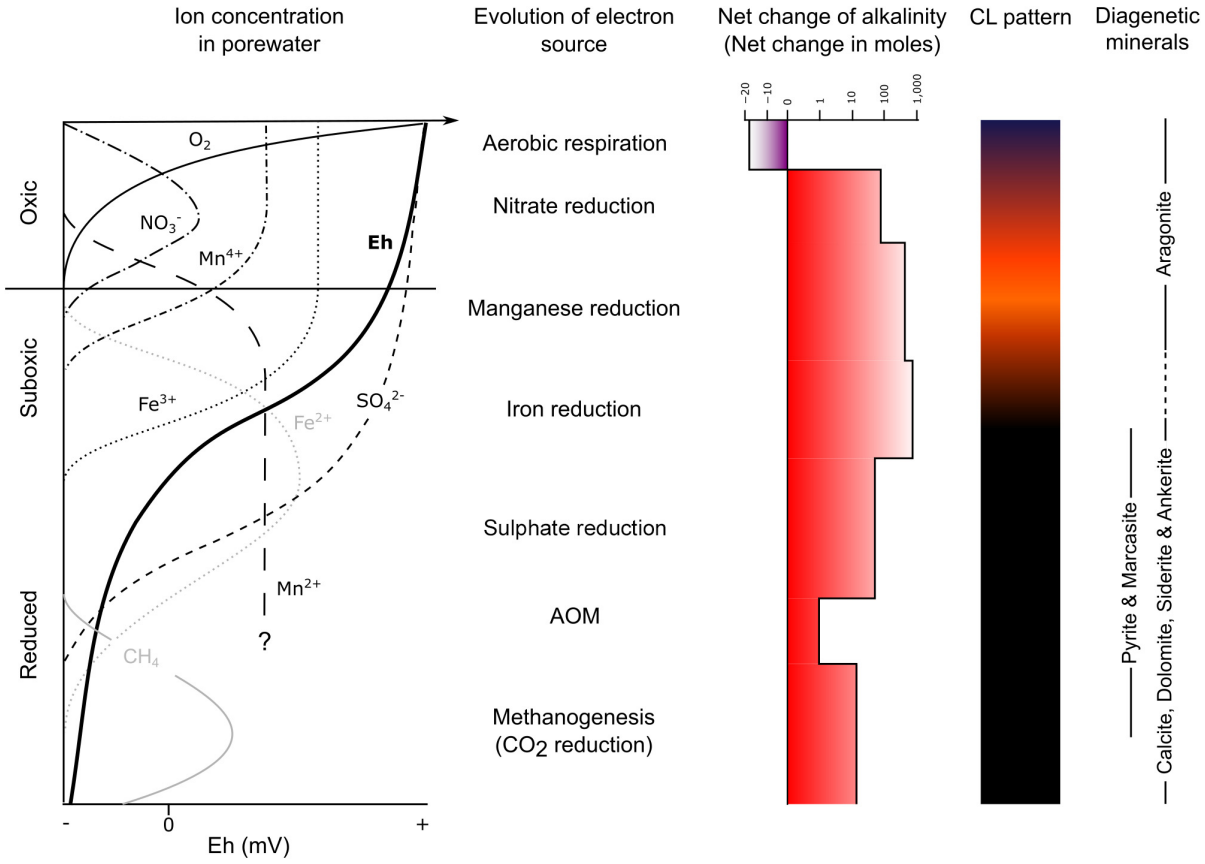

Fig. 3. Evolution of electron acceptor availability, principal metabolic mode (see Table 2), Eh and alkalinity across a depth/redox gradient in marine sediments. Vertical scale varies in accordance with organic matter content and advection rate from millimetres to decimetres. Expected change in cathodoluminescence (CL) intensity of carbonates based on the change in Eh/pH and available ions and known diagenetic mineral phases for each diagenetic zone (Machel, 1985). Modified after Petrash *et al.* (2017).

both the Floridan and the Yucatan modern mixing zones. Its impact is most pronounced where the concentrations of sulphate along the flow paths of deeply circulating fresh groundwater are increased by the dissolution of underlying evaporites (Jones *et al.*, 1993; Sacks & Tihansky, 1996; Socki *et al.*, 2002). In other settings where methane is present, iron and manganese oxides and sulphate stocks can also drive the anaerobic oxidation of methane (AOM, Table 2, Reactions 8a to 8c). When coupled to sulphate, this condition leads to significant regional variability in the sulphate levels of the mixing-zone groundwater (Table 1). The SO_4–AOM is considered a bioenergetically challenging reaction, whereas Mn–AOM and Fe–AOM are more energetically favourable processes (Riedinger *et al.*, 2014). Methane diffused toward suboxic zones can also be oxidized with nitrate (Thiel, 2018). However, in diffusive profiles SO_4–AOM is for the most part more common due to depletion of the other TEA in the vicinity of the methanogenic zone.

The $\delta^{34}S$ values (V-CDT – Vienna-Canyon Diablo Troilite) in the unconfined groundwaters of Central Florida are +1.7 to +33.1‰ for dissolved sulphate and −42.1 to + 14.6‰ for dissolved sulphide. These values likely point to gypsum dissolution as the primary source of the dissolved sulphate that was subsequently reduced in the modern mixing zone (Sacks & Tihansky, 1996). Accordingly, the higher $\delta^{34}S$ values are the product of near thermodynamic equilibrium fractionation between sulphate and sulphide. The lower to intermediate values reflect the

openness of the sulphur cycle and results from other processes occurring in parallel, such as sulphide oxidation and elemental sulphur (S^0) disproportionation: S^0 disproportionation involves the simultaneous reduction of sulphate and re-oxidation of sulphide and is important during shallow burial diagenesis. In anoxic porewater–-sediment systems, it is linked to the reductive dissolution of the Mn(IV)oxide stocks and Fe (III)-(oxyhydr)oxide stocks (Canfield *et al.*, 1998; Böttcher & Thamdrup, 2001) according to Reactions R5 and R6, respectively:

$$S^0 + 3MnO_2 + 4H^+ \rightarrow SO_4^2 + 3Mn^{2+} + 2H_2O \quad (R5)$$

$$3S^0 + 2FeOOH \rightarrow SO_4^{2-} + 2FeS + 2H^+ \quad (R6)$$

Regarding intermediate sulphur availability, Davis & Garey (2018) reported the presence of vents affecting hypoxic cave waters where multicolour biofilms developed. Toward the bottom, the vents sporadically discharge yellowish organic globules containing sulphur-dependent bacteria. Thin filamentous mats with white coatings, presumably elemental S^0, were also found in other parts of the same cave system where fluids sourced from the evaporites underlying the Avon Park Formation admix with the cave waters (Davis & Garey, 2018). This observation exemplifies the complexity of interpreting microbial zonation and functioning, and the role of fluid flow in the transport of TEA within mixing zones.

Recent work on the marine sulphate–methane transition zone (SMTZ) highlighted the importance of microbial sulphate respiration in alkalinity generation (Wurgaft *et al.*, 2019). These findings can be extrapolated to SMTZs developed in coastal aquifers because of the interaction between methane generated in the organic-rich phreatic zone and sulphate-rich mixing zone. Sacks & Tihansky (1996) observed covariation in $\delta^{34}S$ values and HCO_3^-, which were interpreted as indicative of alkalinity generation under a locally significant contribution of microbial sulphate reduction. These authors also mentioned isotopically heavier groundwaters associated with increased sulphate concentrations. However, the $\delta^{13}C$ of dissolved inorganic carbon (−12.0 to −2.9‰) in the Upper Floridian aquifer also suggests methanogenesis and methanotrophy as two significant controls affecting the distribution of inorganic carbon stocks (Table 1).

In the shallow hypoxic mixing zone of the Yucatan Platform, the linking of carbon and sulphur cycles still needs to be fully evaluated. Molecular and isotopic evidence, together with the relative abundance of archaeal communities (Table 3), point to methanogenesis as a dominant process, although with strong control of methanotrophy (Brankovits *et al.*, 2017). Methanogens are strict anaerobes, but apart from that, they are rather versatile with respect to environmental conditions and thrive well within the range of salinities characterizing mixing zones (Thiel, 2018). Based on measurements involving quinone production and consumption, Brankovits *et al.* (2017) estimated that methanotrophs dominate the brackish to freshwater groundwater of the modern unconfined Yucatan aquifer, where they consume up to 93% of the methane produced. This is consistent with a measurable decrease in DOM. Deeper in the aquifer toward the marine interface, Socki *et al.* (2002) suggested a similar syntrophic methanogenesis/methanotrophic mechanism. Those authors observed that the carbon and sulphur cycles are intertwined by correlating shifts in pH and $\delta^{34}S$ of dissolved sulphate and sulphide. Dissolved sulphate measured in the shallow part of the submarine aquifer shifts from +22.2‰ to up to +41.8‰, which Socki *et al.* (2002) interpreted as the result of microbial sulphate reduction. The S isotope shift in sulphate is accompanied by the occurrence of a wide range of isotopically depleted dissolved sulphide (−32.9 to −2.5‰) pointing to a zone of active S cycling that includes re-oxidation and disproportionation. Above this zone, a significant effect on groundwater pH conditions point to the admixture of waters containing $CaSO_{4(aq)}$ derived from the dissolution of underlying evaporites (Socki *et al.*, 2002). Given that the chemical data do not point to removal of sulphate, the methanotrophic process may instead be coupled to nitrate removal (Brankovits *et al.*, 2017), but, as mentioned above, Mn(IV, III) and Fe(III) reduction could also mediate AOM (Beal *et al.*, 2009; Thiel, 2018). Locally, the introduction of more energetic TEA to the AOM zone might be mediated by strong advective flow within the Yucatan aquifer (Canul-Macario *et al.*, 2019).

In the groundwaters of South Andros Island, saturation indices are significantly lower than predicted by theoretical mixing calculations. This is due to *in situ* generation of CO_2 via organic matter oxidation coupled to sulphate reduction (Whitaker & Smart, 1998). As in the

Table 3. Reported microbiome (as determined via 16S rRNA) in Central Florida (Davis & Garey, 2018) and Yucatan (Brankovits *et al.*, 2017) aquifers.

Florida	Yucatan
Methanogenic *Methanobacteriaceae, Methanospirillaceae, Methanococcaceae*	**Methanogenic** *Methanomassiliicoccaceae, Methanobacteriaceae, Methanocellaceae, Methanosarcinaceae, Methanotrichaceae*
Methanotrophic *Methylococcaceae* (*Methylosoma* sp.), *Methylocystaceae*	**Methanotrophic** *Methylococcaceae* *Methylocystaceae*
Methylotrophic *Methylophilaceae* (*Methylotenera* sp.)	**Methylotrophic** *Methylophilaceae*
Ammonia-oxidizing Bacteria: *Candidatus* Anammoximicrobium sp. Archaea: *Nitrosopumilaceae*	**Ammonia-oxidizing** Bacteria: *Nitrosomonadaceae* Archaea: *Nitrosopumilus, Nitrososphaera*
Denitrifying Bacteria: *Rhodocyclaceae, Arcobacter* sp., *Nitrospina* sp., *Sulfurimonas* sp. Archaea: *Halorubraceae, Halobacteriaceae*	**Denitrifying** *Nautiliaceae, Rhodocyclaceae*
Nitrite-oxidizing *Moraxellaceae, Nitrospiraceae*	**Nitrite-oxidizing** *Nitrospinaceae, Nitrospiraceae*
Sulphate-reducing *Desulfatibacillum* sp., *Desulfotalea* sp., *Desulfosarcina* sp., *Dissulfuribacter* sp., *Desulfocapsa* sp.	**Sulphate-reducing** *Desulfobacteraceae, Desulfobulbaceae, Syntrophaceae, Syntrophobacteraceae*
Sulphur-oxidizing *Sulfurimonas* sp., *Thioalkalispira* sp., *Arcobacter* sp., *Thiobacillus* sp., *Alkalilimnicola* sp.	**Sulphur-oxidizing** *Rhodocyclaceae, Helicobacteraceae, Ectothiorhodospiraceae, Halothiobacillaceae, Thiotrichaceae*
Unknown *Emcibacteraceae*	**Multiple** *Hydrogenophilaceae*

case of the Yucatan aquifer, the zone of dissimilatory sulphate reduction and organic matter oxidation in the subsurface of South Andros Island is separated by a redox interface from an overlying zone of sulphur species re-oxidation. This interface is an important locus for carbonate mineral dissolution (Lasemi *et al.*, 1989). Yet, the combined product of enhanced groundwater flow, source mixing and OM oxidation is ultimately favourable to dolomite growth (Whitaker & Smart, 1998). Dolomitic crusts form in Ambergris Cay, Belize, a sedimentary setting that can be described as a coastal aquifer where admixture of freshwater and seawater occurs (Mazzullo *et al.*, 1987; Teal *et al.*, 2000). The dolomitic crusts here formed under the influence of seasonally fluctuating salinities which also indicates complex mixed-water interactions. The $\delta^{13}C$ and $\delta^{18}O$ data from these dolomitic crusts point to the influence of meteoric waters transporting soil-derived carbon through the flats (Mazzullo *et al.*, 1987; Teal *et al.*, 2000). In schizohaline settings, sulphur-dependent metabolisms were also proposed as key agents capable of buffering the system toward a sustained state marked by elevated pH and alkalinity generation (Petrash *et al.*, 2016). Notably, in the Pleistocene of the Abu Dhabi sabkha, where brackish groundwater with a meteoric influence admixes with partially evaporated seawater,

sulphur-respiration appears to also be an important driver of cementation by partially ordered, near stoichiometric dolomite in the sediment column of the upper intertidal zone (Chafetz *et al.*, 1999; Geske *et al.*, 2015).

Thus far, there has been consideration of geological and hydrochemical evidence suggestive of mixing zones as dynamic regions of the biosphere where the unique functional attributes of subsurface microbial life combine to produce an environment that may be favourable to dolomite precipitation. The following section provides an updated biogeochemical perspective to mixing-zone dolomitization.

REVISED BIOGEOCHEMICAL MIXING-ZONE DOLOMITIZATION MODEL

From the commonalities shared by the dissimilar examples above, the picture that emerges is that coastal mixing zones display marked geochemical disequilibrium interfaces in which oxidizing and reducing species coexist and can be utilized multiple times by diverse prokaryote communities. The disequilibrium interfaces are movable diagenetic fronts in which discrete biogeochemical reactions with an impact in mineral saturation occur within enclosed pore spaces that are also affected by advective mixing of fluids with contrasting composition and redox potentials. In their dynamic niches, the microorganisms fuelling such reactions induce large-scale transformations of buried OM and have an attendant impact on the long-term C cycle (Edwards *et al.*, 2012; LaRowe & Amend, 2015; Scheller *et al.*, 2016). This impact includes OM remineralization and carbonate mineral dissolution and (re)precipitation, with dolomite being the most thermodynamically stable product.

There is a general lack of systematic genomic analyses targeting gene and functionalities expression along hydraulic and redox gradients of modern coastal aquifers. Yet, the distribution and relative abundance of subsurface microbes in the mixing zones of Florida and the Yucatan have been evaluated independently by using prokaryotic 16S ribosomal RNA gene (16S rRNA) analyses (Brankovits *et al.*, 2017; Davis & Garey, 2018). These authors focused on the water at different salinity of cave systems to provide insight into biogeochemical processes in the coastal mixing zone. In both carbonate platforms, the microbial community structure varies with chemical stratification, and is spatially heterogeneous. Despite marked differences in the chemical features of the Floridian and Yucatan aquifers – a fact first highlighted by Back & Hanshaw (1970) – there is a remarkable similarity amongst the communities and potential functionalities represented by the prokaryotes thriving in the mixing zones of both settings (Table 3). Limited genomic analyses prevented species-level identification and inferences of their exact metabolic functioning. Yet, by using a comparative bioinformatic approach relying on high quality sequence marker-gene analysis and comparison with sequences deposited in gene-accession banks, methanogenesis, methanotrophy sulphur disproportionation, and sulphate reduction appear as dominant pathways in the anoxic part of the mixing zone (Brankovits *et al.*, 2017; Davis & Garey, 2018). As revised and discussed in Petrash *et al.* (2017), such metabolic pathways, together with the heterotrophic breakdown of Ca-reactive and Mg-reactive EPS, have been linked to near-surface dolomite formation, and may also facilitate dolomitization in low temperature (<60°C) burial diagenetic realms.

The formation of dolomite in a coastal mixing zone requires a mechanism for Mg^{2+} (and Ca^{2+}) delivery, dehydration of aqueous complexes and a set of conditions promoting nucleation of new dolomite crystals and/or stabilization of pre-existing precursors as dolomite. In the case of the latter, subsurface microbes could facilitate dolomitization through: (i) the production of exopolymeric biomacromolecules with strong affinity for Ca and Mg cations and templating properties (Warthmann *et al.*, 2000; Bontognali *et al.,* 2010; Zhang *et al.*, 2012b); (ii) efficient generation of alkalinity linked to OM respiration processes and Fe and Mn cycling (e.g. Petrash *et al.*, 2015, 2016a, 2016b); (iii) release of dissolved sulphide through bacterial sulphate reduction (Zhang *et al.*, 2012a); and (iv) the availability of transition metal catalysts (Daye *et al.*, 2019; Vandeginste *et al.*, 2019). The mixing zone represents an environment where the conditions listed above can locally concur for periods of 10^4 to 10^5 years while the biogeochemically controlled diagenetic front transitions upward and downward through the sediment pile in response to recurrently changing agents, such as climate, hydrology and glacioeustacy (Saller *et al.*, 1994; Csoma *et al.*, 2004). Therefore, the revised biogeochemical mixing-zone dolomitization model discussed here (Fig. 4), portrays coastal mixing zones as domains where carbonate diagenesis is

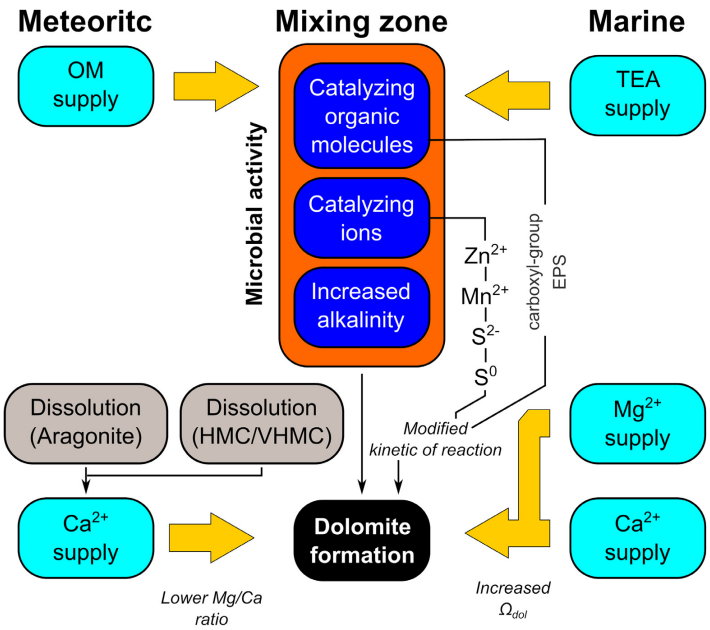

Fig. 4. Conceptualization of the revised mixing-zone diagenetic model considering the biogeochemical controls over dolomitization.

influenced by the sedimentary supply of OM and the presence of regenerable TEA that fuel an active subsurface life.

Subsurficial microbial activity may also control the OM stocks, with variable rates and types of autotrophic and heterotrophic reactions that could significantly modify the pCO_2 levels, driving dissolution/reprecipitation processes. In parallel, the high concentrations of Ca^{2+} from the dissolution of metastable aragonite and calcites, and a constant supply of Mg^{2+} from circulating marine waters and from the dissolution of VHMC, locally results in oversaturation with respect to dolomite. In this diagenetic front, the known kinetic barriers limiting the formation of dolomite are diminished by microbes (Sumrall *et al.*, 2015). Moreover, as the mobile dolomitizing front reaches stratigraphic levels with a uniform density of pre-existing dolomite nuclei, it can effectively contribute to stabilize these as a cement or as a replacement phase, leading to dolomitization. The pre-existing nuclei likely formed syngenetically or early during diagenesis of reef (e.g. Mitchell *et al.*, 1987) to peritidal settings (e.g. Teal *et al.*, 2000) under the influence of seawater. To then account for the large-scale dolomite cementation and/or replacement that typify some levels in Neogene to Palaeogene platforms, the dolomite precursors must have passed through multiple palaeo-mixing zones. This is because throughout any given carbonate platform, at timescales of 10^5 to 10^6 years, the mixing zone and its intrinsic diagenetic processes migrate back and forth as the result of relative sea-level change and coastal progradation and retrogradation (Csoma *et al.*, 2004), which repetitively expose most of the upper part of the platform to contrasting biogeochemical conditions. Migration of the redox front and reoccurrence of the mixing zone over such timescales could theoretically result in a large dolomite body (Humphrey & Quinn, 1989; Budd, 1997).

As discussed in the next section, in some cases the fabric in the younger mixing zone, predominantly replacing dolomite is retentive, suggesting a nuanced dissolution–precipitating reaction at the crystal surface level. Local microenvironments and surface reactive components related to microbial activity may play a significant role in allowing this sort of cementation and replacement mechanism. The importance of microenvironments stands out even more when arid environments are concerned as the organic load in them is lower and localized. Still, under arid precipitation conditions, both the mixing of fluids with contrasting salinity

and locally variable biogeochemistry could be related to dolomitization, as observed in sabkha environments (Chafetz *et al.*, 1999; Geske *et al.*, 2015; Rivers & Kaczmarek, 2020).

PETROGRAPHIC AND GEOCHEMICAL FEATURES OF DOLOMITE AS BIOGEOCHEMICAL MIXING-ZONE PROXIES

Diverse chemical and microbial parameters can be measured in modern mixing zones, but such measurements only reflect a short, somewhat static, view of a temporally and spatially variable picture. The 'snapshots', however, can be recorded in the carbonate rock record either as a time series, i.e. multiple generations of cements with discrete chemical and isotopic signatures, or an integration of them over time. As discussed in this section, this implies that the cements and recrystallized carbonates formed in equilibrium with porewaters in the mixing zone also record changes in climate and relative sea level over multiple temporal timescales. Those externally driven secular changes present challenges to extrapolating through time and space all possible biogeochemical and redox transformations occurred in mixing zones. On the other hand, dissolution voids and non-recrystallized mineralogical products produced along these cycles are often preserved and can inform us on the changes in the palaeochemistry of the aquifer relative to the migration of the mixing zone.

A link between carbonate diagenesis and sea-level changes has been previously referred to by Csoma *et al.* (2004) as diagenetic salinity cycles. The definition of such cycles is useful for predicting early near-surface diagenetic processes and products, given a record of relative sea-level rise and fall and accompanying shallow burial alteration under the set of conditions pertaining to the mixing zone (as was previously described by Matthews & Frohlich, 1987; Humphrey & Quinn, 1989). Csoma *et al.* (2004) suggested that, beginning with deposition, coastal carbonate rocks could be bathed in successive cycles of marine phreatic, mixing zone, freshwater phreatic, mixing zone and marine waters as sea level oscillated through time (Fig. 5A to D). The marine to freshwater leg occurs with sea-level fall, and the freshwater back to marine leg occurs with sea-level rise. These salinity cycles are superimposed by climatic shifts driven by eccentricity, and more frequently by precession and obliquity forcing mechanisms (Fig. 5E). The climatic shifts modify the freshwater recharge, evaporation and vegetation patterns, with concurrent effects over the diagenetic potential in freshwaters and mixing zones (Saller *et al.*, 1994).

A long-term proxy is required to understand how the temporal and spatial changes in the bioavailable energy sources associated with a diagenetic salinity cycle might be manifested in a dolomite body. A way forward is through detailed analyses of well-preserved zoned dolomitic carbonate cements that were stabilized under the influence of ancient mixing zones. The traditional mixing-zone interpretation of most of these cements is typically based on bulk rock $\delta^{18}O$ values that are less than those of contemporary dolomite formed from seawater, and/or exhibit a linear covariance with $\delta^{13}C$ values, suggestive of the influence of carbon transformations not associated with marine pore fluids. Critics of the traditional mixing-zone model would reject these arguments, suggesting instead flawed interpretation of $\delta^{18}O$ values. In doing so, they disregard variation in *in situ* temperatures and fluid composition. In addition, there is large uncertainty regarding the actual $\delta^{18}O$ fractionation factor between the fluid source and dolomite (Müller *et al.*, 2019). Depending on what factor is used, variability of $\delta^{18}O$ estimated for the water in equilibrium with the mineral at the time of precipitation can exceed 3‰ (Murray & Swart, 2017). Despite uncertainty, a review of the isotopic attributes of these cements is nonetheless informative as it sheds light on what the ultimate product of a mixing-zone dolomite might be. Further, as detailed in a subsequent section, these presumed mixing-zone products would be the ideal proxy in which to assess new analytical methods for the assessment of a mixing-zone origin of dolomite.

The dolomites that are most confidently associated with mixing zones are characterized by multiple generations of cements exhibiting complex, yet similar mineralogical, textural and *in situ* chemical features. For instance, the mixing-zone cements in the upper part of the Eocene Avon Park Formation, originally described by Cander (1994), appear in the matrix of a previously formed fabric destructive replacement dolomite (Fig. 6A). The cements consist of two generations of syntaxial dolomite that often encircle multiple replacive crystals. The cements exhibit variable Fe and Mn compositions, as observed via cathodoluminescence

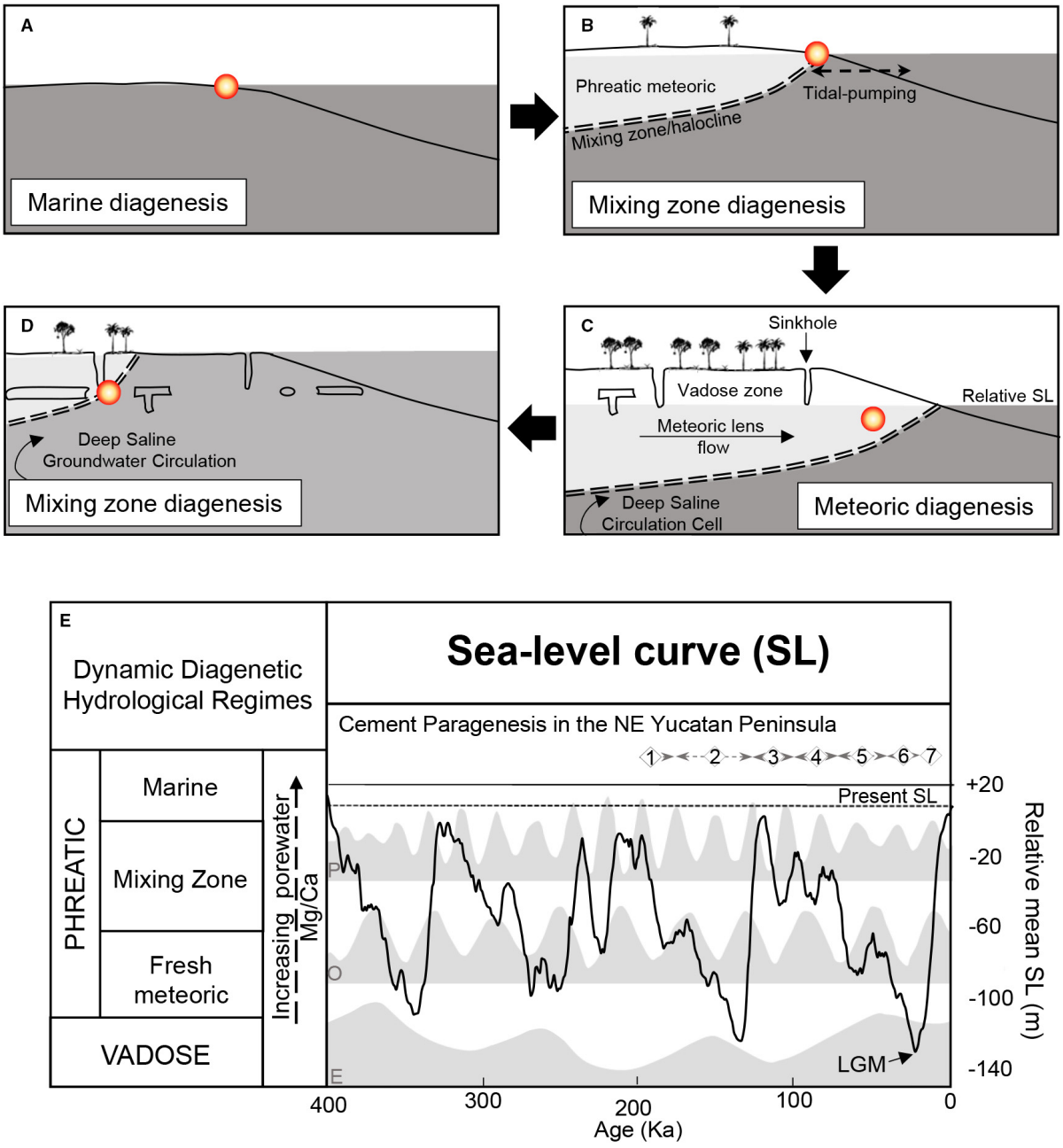

Fig. 5. Schematic diagram illustrating the early diagenetic evolution of the late Pleistocene reefal limestones of the Yucatan Peninsula. Early diagenesis (marine, meteoric and mixing zone) of these rocks is controlled by changes in sea-level: (A) marine; (B) mixing zone; (C) meteoric; and (D) mixing zone. (E) Through time, the early diagenetic events include: (1) micrite envelopes and submarine cementation in the marine environment; (2) loss of Mg-calcite, precipitation of sparry calcite cement, neomorphism and dissolution of aragonite in the mixed and freshwater environment; (3) dolomitization (replacement and cementation) and aragonite dissolution in the mixing zone; (4) precipitation of zoned dolomite cements in the mixing zone; (5) precipitation of calcite cements in the freshwater environment; (6) dissolution of high-calcium dolomite and Mg-calcite cements in the freshwater environment; and (7) intercalation of dolomite and calcite overgrowths or Ca-dolomite. Composite Pleistocene sea-level (SL) stack after Spratt & Lisiecki (2015) with eccentricity (*ca* 100 kyr), obliquity (*ca* 41 kyr) and precession (*ca* 21 kyr) frequencies illustrated in the shaded curves; LGM – Last Glacial Maximum. Modified from Ward & Halley (1985).

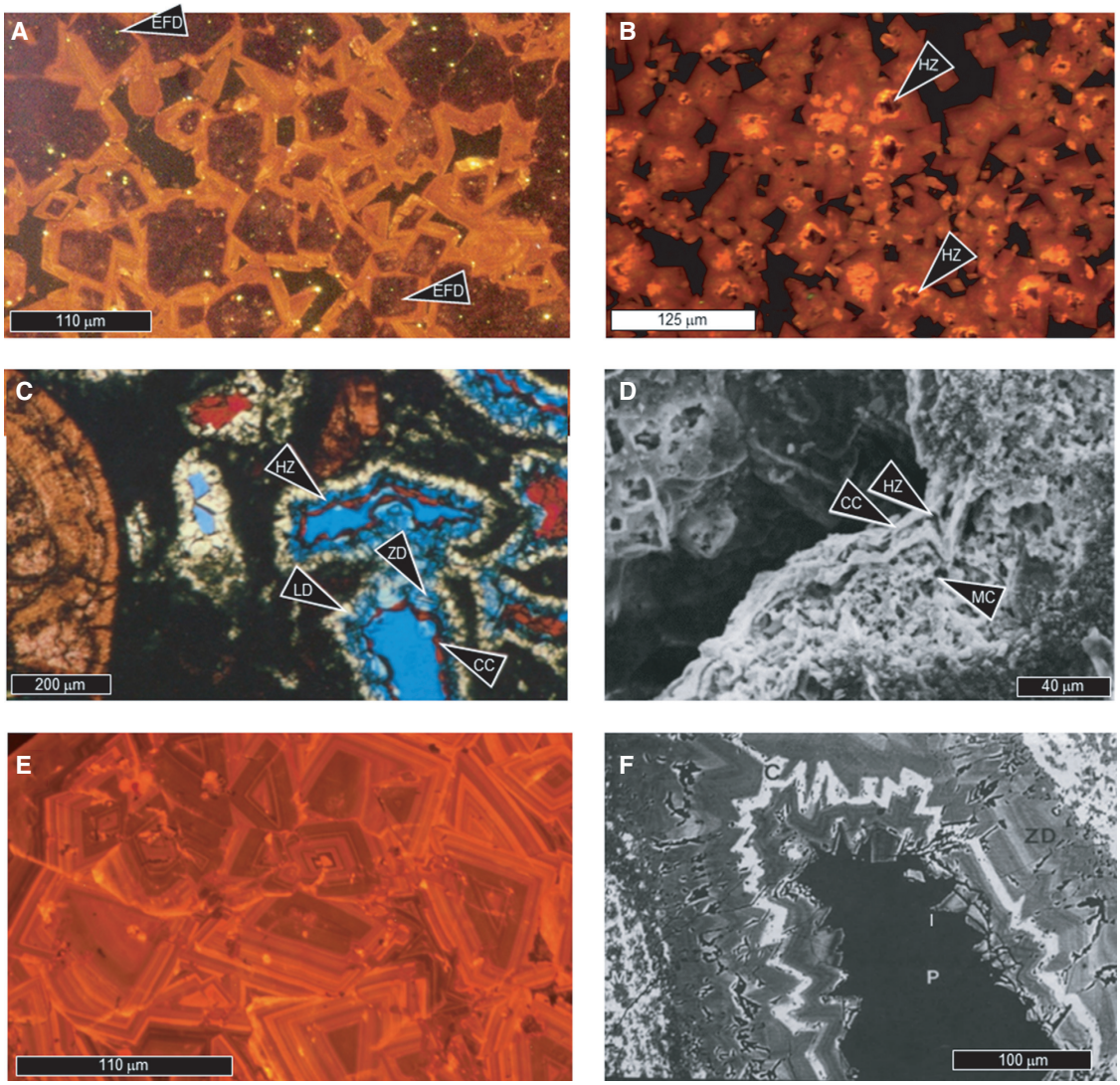

Fig. 6. Petrographic features of dolomite interpreted as mixing-zone products. (A) Cathodoluminescence (CL) image of Late Eocene Avon Park Formation, Florida (core TR8-1 from well W-15826, −306.9 m). Early formed, inclusion-rich, non-cathodoluminescent cores of marine dolomite – EFD (arrows) are enveloped by layered luminescent mixing-zone dolomite cements characterized by alternating layers of dolomite and calcite. (B) CL image of Oligocene Ocala Formation, Florida (Well 17 056, −343.8 m; modified from Gaswirth *et al.*, 2007) illustrating bright luminescent dolomite cement formed atop older marine dolomite with dull red luminescence, hollow zones – HZ (arrows). (C) Late Pleistocene of north-eastern Yucatan (Core K-274 near Pedregal, −4.1 m; modified from Ward & Halley, 1985) coral mould with dolomite and calcite cements. Moulds are lined with limpid dolomite – LD, which is enveloped by zoned dolomite – ZD. Note also hollow-zoned crusts – HZ composed of calcite cement – CC. Plane polarized light; Alizarin Red S stained; porous space filled by blue epoxy. (D) Late Pleistocene of north-east Yucatan (Core K-274 near Pedregal, −5.1 m; Ward & Halley 1985). Detail of hollow-zoned calcite cements shown in (C). The SEM photomicrograph shows well-preserved outer CC layers, and hollow layers – HZ, presumably representing partially dissolved Ca-dolomite. Partially dissolved inner zone presumably composed of Mg-calcite (MC). (E) Miocene dolomite, Seroe Domi Formation, Curaçao (sample from the Seru Prekstul outcrop of Fouke *et al.*, 1996), showing concentric CL zones and sectorial zoning. (F) Late Pleistocene reef terrace at Golden Grove (southeastern Barbados; modified from Humphrey & Radjef, 1991). The pore-filling cement sequence is shown in BSEM. Cements nucleate on partially dolomitized matrix – M, and include compositionally zoned dolomite – ZD and syntaxial calcite band (C) and grow into primary pore spaces (P). (C) and (D) Reproduced with permission from SEPM (*J. of Sed. Res.*). (F) Reproduced with permission from Elsevier B.V. (*Sed. Geol.*).

(Cander, 1994; Choquette & Hiatt, 2008), which points to precipitation in equilibrium with porewater of variable, and cyclic redox states (Cander, 1994; Choquette & Hiatt, 2008).

In the Eocene Ocala and Oligocene Suwannee formations, Gaswirth *et al.* (2007) reported luminescently zoned dolomite similar to that present in the underlying Avon Park Formation. In the Suwannee Formation the dolomite is also a syntaxial cement (Fig. 6B); in the Ocala Formation, the dolomite phase is a partially neomorphic alteration of the original replacive dolomite (Fig. 6C, Gaswirth *et al.*, 2007). The authors attributed both types of luminescent dolomites to exposure for considerable time of the respective rock units to high $\Omega_{dolomite}$ mixing-zone groundwater in a confined aquifer. Modelling of the Sr isotopic composition of the Suwannee and Ocala dolomites indicated that the luminescent phases formed at separate times in the Neogene in response to sea-level and climatic change (Gaswirth *et al.*, 2007). Thus, the differences in the petrographic features and luminescence of the Avon Park, Ocala and Suwannee luminescent dolomites may result from variation in space and time of the geochemical processes and conditions in the three different mixing-zone systems.

In the Yucatan Platform, Ward & Halley, 1985; Fig. 6D) reported that dolomite occurs as a finely crystalline, anhedral to subhedral phase (3 to 15 μm) that replaces host-rock matrix of packstone and wackestone, typically leaving calcitic skeletal fragments undolomitized. Dolomite also occurs as a complexly zoned cementing phase that consists of subhedral rhombs 20 to 100 μm in size, followed by a zoned, 2 to 10 μm thick layer of syntaxial dolomite. The dolomite exhibits compositional Mg/Ca variabilities and may also alternate with calcite layers (Fig. 6E). The alternating calcite is either low (1 to 3 wt.%) or high (4 to 7 wt.%) Mg-calcite that was interpreted to have formed in the dilute portion of a palaeo-mixing zone. The Mg-calcite cements are partially to totally leached, and Ca-dolomite layers are often dissolved, forming hollow-zone crystals. Notably similar textural features have been reported and interpreted as mixing-zone products in Neogene rocks of multiple Caribbean settings. Examples include the Mio-Pliocene Seroe Domi Formation of Bonaire and Curaçao (Sibley, 1980, 1982; Fouke, 1994; Lucia & Major, 1994; Sumrall *et al.*, 2016; Fig. 6E), in a late Pleistocene reef terrace of Barbados (Humphrey, 1988; Humphrey & Kimbell, 1990; Humphrey & Radjef, 1991; Fig. 6F) and in the Miocene Cayman Formation of Grand Cayman where Jones and coworkers, carefully documented the textures and geochemical signatures associated with mixing-zone dolomite (Jones, 1989; Zhao & Jones, 2012; Ren & Jones, 2017, 2018). Sumrall *et al.* (2015) also reported dolomite wall rock in caves of Isla de Mona (Puerto Rico) that were polygenetic (replacement plus subsequent cement). A younger euhedral rhombic carbonate cement phase with near equal proportions of Mg and Ca (undetermined if dolomite or VHMC) also encase microbial filaments within the wall rock, suggesting a microbial influence in at least those dolomite crystals. However, these delicate fabrics rarely appear to be preserved in the sedimentary record due to a combination of Ostwald ripening, dissolution–reprecipitation and overgrowth.

In those examples not related to a confined aquifer, aqueous dissolution and reprecipitation processes are also indicated; one that involves partial dissolution of relatively unstable submicron scale Ca-dolomite and VHMC precursors (Gregg *et al.*, 2015), accompanied by growth of a more stable form of dolomite, for example, finely crystalline rhombs followed by their overgrowths. The precipitation mechanism seems to lead to the next diagenetic sequence. Following the initial deposition (Fig. 7A) and early alteration of the sediment (Fig. 7B and C), at the first stage (Fig. 7D) limpid euhedral–subhedral Ca dolomite/VHMC crystals (20 to 100 μm in size) are formed. These are followed (Fig. 7E) by dolomite with zones formed by variations of the calcium/magnesium ratios, variable and usually alternating Mn and Fe contents. Finally, generations of alternating calcian dolomite and calcite cement and a thin rim of calcite cement develop as a cortex (Fig. 7F). The second stage of this sequence indicates a strong control by changes in the redox potential over the solubility and precipitation potential of VHMC and Ca-dolomite. These changes are driven by both changes in the supply of DOM and TEA, which, in turn, implicate the activity of subsurface microbes that utilize them. As relative sea level fluctuates, some of the more reactive phases formed along this cycle might be dissolved, resulting in hollowed out crystals (Kyser *et al.*, 2002). This porosity may be filled by later generations of cement and obscure the temporal order of the cement stratigraphy (James *et al.*, 1993; Jones, 2007). However, in some cases, initial dolomitization can occur in other settings (Fig. 7G) and

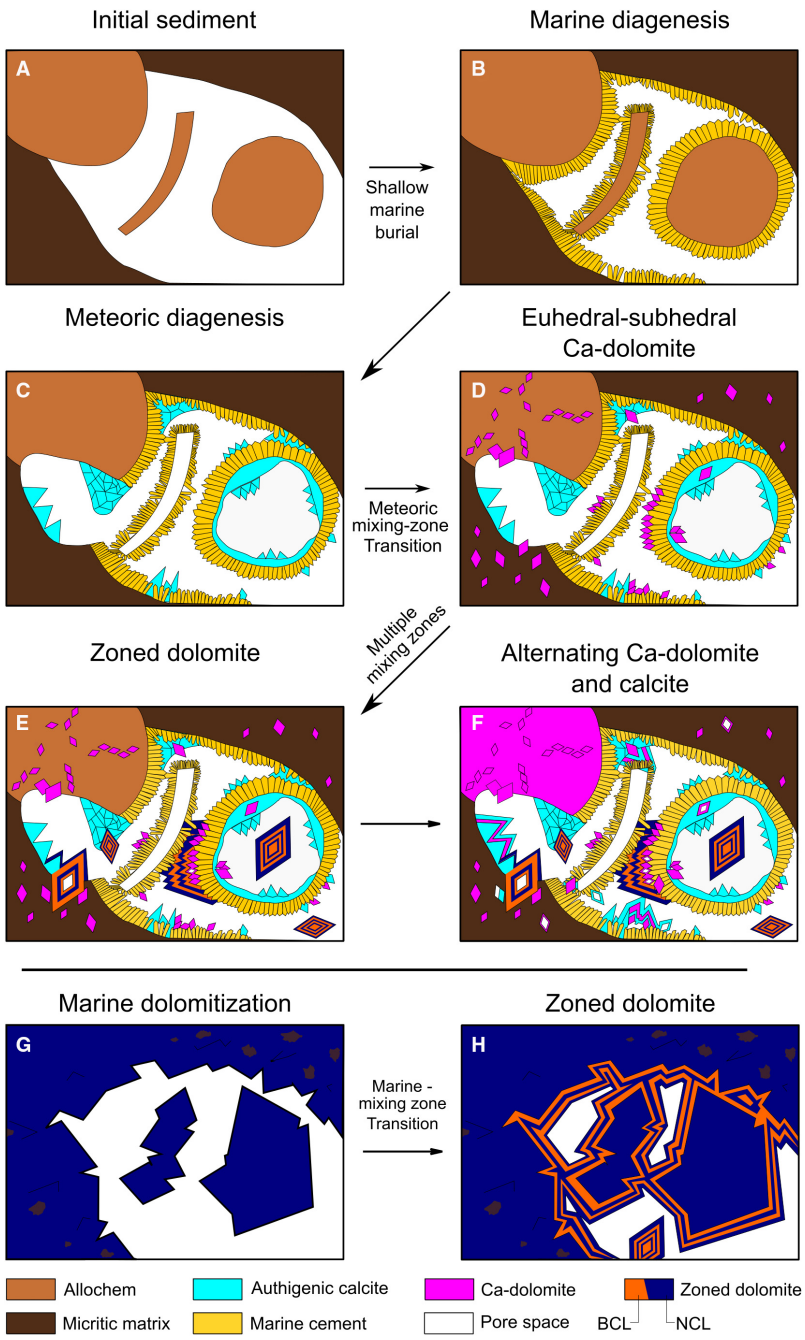

Fig. 7. Scheme illustrating an idealized sequence of cement growth in relation to mixing-zone dolomite. Starting with an (A) open pore bounded between allochems and micrite formed, this pore would be filled with fibrous to bladed aragonitic cement under marine conditions (B). However, with exposure to meteoric waters preferential dissolution and replacement of very high-Mg calcite (VHMC) and aragonite (C) follows, although non-selective dissolution might also occur in extreme cases of undersaturation (for example, meteoric vadose). Upon introduction to the active zone of mixing, first limpid Ca-dolomite/VHMC grows (D), followed by zoned dolomite overgrowths (E), with partial dissolution of Ca dolomite and/or VHMC. In the final stage (F), more stable dolomite can be intercalated with calcite overgrowths or Mg-enriched, Ca-dolomite. Initial dolomitization may occur in the marine environment (G) and be then introduced to the mixingzone (H), where pore filling zoned dolomitic cement (as overgrowth) would form. BCL (bright luminescence) and NCL (no luminescence) refer to appearance under CL microscopy.

would be followed mainly by the zoned cements (Fig. 7H) – as is the case in the Avon Park Formation (Cander, 1994).

The above ideal paragenetic sequence is not present in its entirety in many cases. This may, in part, reflect the complexity of a given palaeo-mixing-zone's hydrological path and susceptibility to short-term transient changes in climate and flow patterns. Whitaker *et al.* (1994), for example, noted that most of the likely mixing-zone dolomites in the Bahamas Blue Hole were not zoned and likely formed within a brief period within one of the above stages. On the other hand, those mixing-zone dolomites interpreted as the product of confined Palaeogene aquifers (for example, Avon Park, Ocala and Suwannee formations) are characterized by just the zoned dolomite. This likely reflects the confined nature of their parent aquifer – the confinement would have meant less susceptibility to short temporal fluctuations in redox conditions, microbial activity and climatic (recharge and sea-level change) conditions. In contrast, the unconfined Pleistocene coastal aquifer systems (for example, Barbados and Yucatan) tend to exhibit all components. In the Yucatan, Ward & Halley (1985) consider the complete sequence presented to reflect progressive freshening of groundwater during the initial stage of a late Pleistocene fall in relative sea level (Fig. 6E).

In the examples in which precursor dolomite played a key role, the precursors within each unit also had different solubilities depending on crystal size, shape and texture (Nielsen *et al.*, 1994), but also on their Mg:Ca ratio. Migration or generation of fluids with high pCO_2 can result in differential dissolution along the crystallite surfaces starting with the most thermodynamically unstable Mg-calcites, then aragonite and poorly ordered Ca-dolomite phases. This dissolution sequence may have two ongoing effects. The first is calcite reprecipitation due to the common ion effect, which will cause a slight increase in the fluid's Mg:Ca ratio that would favour the formation of more ordered Ca-dolomite (Ren & Jones, 2018). The second effect would be formation of confined microenvironments that may prompt formation of Mg-rich amorphous calcium carbonate (Jiang *et al.*, 2011), which would then be a precursor for additional Ca-dolomite. As unstable dolomite precursors are dissolved within the dynamic precipitation environment, the hybrid porewaters may also become supersaturated with respect to dolomite and the process of precipitation of more stable crystals could proceed under higher alkalinity conditions.

The common denominator in the interpreted mixing-zone processes considered here is cements. These cements may exhibit complex zonation consisting of compositional Mg/Ca variabilities and, in some cases, calcite–dolomite alternations. The intercalated calcite cement layers may be related to calcification of a biofilm developed in the pore spaces at times when the dolomitized level was affected by chemical fluctuations in porewater that decreased the dolomite precipitation rates, thus allowing the faster kinetics of calcite to transiently govern cementation. The petrographic evidence shows that crystals nucleate on pre-existing crystal surfaces and grew as either entirely new crystals or by continued growth around earlier-formed fine crystalline precursors. Importantly, compositional and mineralogical heterogeneity in mixing-zone dolomites (for example, Fig. 6) impose limitations to bulk carbonate rock geochemical and isotopic datasets that rather represent averages for multiple events. Small variations in the redox states of the porewater–sediment system at the time of crystal growth could influence the C and O isotope ratios and the content of redox sensitive elements, such as Mn and Fe, at the crystal scale. Emergent methods that would resolve the *in situ* variability discussed in this section, and the relevance of these, and other methods for future interpretations of mixing-zone dolomites are discussed below.

DETECTING BIOGEOCHEMICAL SIGNATURES OF MIXING-ZONE DOLOMITES

Testing the revised diagenetic mixing-zone dolomitization model requires evaluating the presence of biogeochemical tracers and proxies that can be affected by the dynamics of mixing-zone processes. Future research efforts thus should rely on both traditional and emerging techniques that can reveal new insights into biogeochemical reactions relevant to the formation of ancient authigenic dolomite phases, which requires reassessing the interpretation of traditional proxies. Those approaches can also be used to re-examine the examples of interpreted mixing-zone dolomites described above, and thus establish whether they are indeed mixing-zone products. This last section presents the framework for such analyses with a focus on

trace elements, luminescence patterns and geochemistry of multiple isotope systems.

Trace elements and cathodoluminescent signatures

As discussed in prior sections, dolomite cements precipitated in mixing zones typically exhibit complex cathodoluminescence (CL) patterns indicative of biochemically driven shifts in Eh and divalent Fe and Mn availability. Over longer periods, changes in the mixing-zone position (for example, Fig. 5) would modulate the DOM and TEA availability in each stratigraphic location as a function of mixing-zone migration. The resulting carbonate formed in the seaward portion of the mixing zone would likely be non-luminescent (Machel *et al.*, 1991) with possible thin luminescent rims reflecting a transient redox state where dissolved Fe was lower than dissolved Mn (Gies, 1975; Machel, 1985; Budd *et al.*, 2000). In mixed porewaters containing by-product HS^-, however, the relative Mn concentrations might increase significantly as Fe precipitates in pyrite precursors, but, in general, the dissolved Mn ions are usually much less than aqueous Fe concentrations (for example, $\leq$2 μM of Mn^{2+} versus $\geq$100 μM of Fe^{2+}; Table 1). It has also been suggested that Zn, another biosensitive element, may sensitize Mn-activated luminescence (Gies, 1975; Machel, 1985), and thus may play a part in the complex CL zonation of mixing-zone dolomite cements (but see Budd *et al.*, 2000).

The intracrystalline distribution of these elements has been shown to correlate to different $\%MgCO_3$ bands of dolomite cements interpreted as mixing-zone products (Kyser *et al.*, 2002). Other potential trace metal CL modifiers, such as Co, Ni (Machel, 1985) or Ce (Habermann *et al.*, 1996), are also sensitive to changes in redox states and might contribute to CL zonation. The initial release to porewaters of redox sensitive elements, such as Ce, that can contribute to chemical zonation in dolomite crystals formed under predominantly anoxic, schizohaline conditions has been linked to the biogeochemical reductive dissolution of Fe-(oxyhydr) oxides and Mn-(oxyhydr)oxides (Petrash *et al.*, 2016a,b). High spatial resolution and precision techniques that can systematically advance the understanding of these metals and their role in CL zonation of mixing-zone dolomites are now readily available (for example, ion and photon probes, notably synchrotron-based X-ray absorption and fluorescence). Evaluating the spatial distribution of those trace elements would serve as an additional test of the biogeochemical mixing-zone dolomite model.

Isotopic geochemistry

Much of the debate first establishing and then refuting the original mixing-zone dolomitization model stems from interpretation of stable O isotope data (e.g. Land, 1991, Melim *et al.,* 2004). However, most of the currently available isotopic analyses of dolomite interpreted as formed in the mixing zone are based on whole-rock powders of what is presumed to be pure dolomite, or chemically separated dolomite fractions from mixed-mineralogy limestones (e.g. Swart & Melim, 2000). The individual dolomite crystals are typically complexly zoned (precursor dolomite plus syntaxial cements) and, thus, their bulk isotope contents represent the integration of variable geochemical conditions during crystal growth. Therefore, the stable isotope values considered here likely average discrete equilibrium processes occurring in porewaters of temporally varied composition. These groundwaters were seawater and admixtures of seawater and meteoric waters, all with dissimilar organic contents, $\delta^{13}C$ and $\delta^{18}O$ values. Despite this fact, compared to Plio-Pleistocene Caribbean dolomite formed dominantly from seawater (Higgins *et al.*, 2018, and references therein), nearly all Late Cenozoic examples of dolomites from the Caribbean Sea and the Gulf of Mexico that are interpreted as mixing-zone products exhibit lower $\delta^{18}O$ and $\delta^{13}C$ than their marine counterparts (Fig. 8).

The stable C and O isotopes of mixing-zone dolomites exhibit two potential trends (Fig. 8). One of co-depletion of ^{18}O and ^{13}C (with a slightly stronger decrease in $\delta^{13}C$ values) and the other dominated by depletion in ^{13}C accompanied by only a minor decrease in ^{18}O. Diagenetic models of meteoric–seawater mixing zones presented by Zhao *et al.* (2020) show that the relationship between $\delta^{13}C$ and $\delta^{18}O$ values can be variable as sediments recrystallize. This can be driven either by physical mixing of the fluids, which shows a high degree of covariance, or the gradual re-equilibration of carbonate minerals with diagenetic fluids, which can vary due to preferential rock-buffering of carbon isotopes compared to oxygen isotopes. The co-depletion of carbon and oxygen isotopes has long been interpreted as a freshwater–seawater mixing

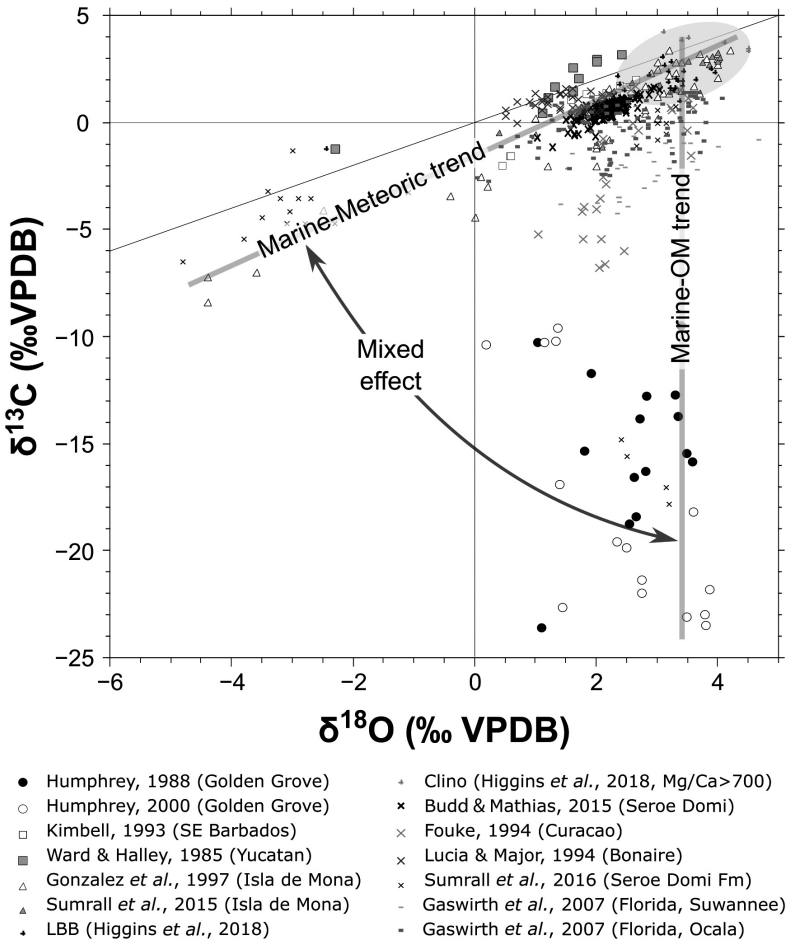

Fig. 8. $\delta^{18}O$ versus $\delta^{13}C$ cross-plot of Neogene dolomites including those attributed to a mixingzone (Ward & Halley, 1985; Humphrey, 1988, 2000; Kimbell, 1993; Fouke, 1994; Lucia & Major, 1994; González *et al.*, 1997; Gaswirth *et al.*, 2007; Budd & Mathias, 2015; Sumrall *et al.*, 2015, 2016) and marine dolomites of the Bahamas (Higgins *et al.*, 2018, and referances therein). Two main trends are visible and define mixing lines to the marine end member. One is a marine–meteoric covariance in $\delta^{18}O$ and $\delta^{13}C$ to values like those in freshwater systems. The second is a $\delta^{13}C$ trend created by biogeochemical alteration of marine organic matter (OM) toward lowest $\delta^{13}C$ values ascribed to methane oxidation. Most of the data points related to dolomites interpreted as mixing-zone products fall between these two trends, suggesting a mixture of both components. VPDB, Vienna Pee Dee Belemnite.

trend (Allan & Matthews, 1982), with the decreasing $\delta^{18}O$ values associated with increasing percentages of meteoric water in mixing zones, and the decreasing $\delta^{13}C$ values driven by increasing influence of soil-respired ^{12}C in that meteoric water (Lohmann, 1988). More recently, however, Swart & Oehlert (2018) interpreted such covariance as the result of diagenetic processes occurring to varying degrees within the interface between vadose and phreatic zones as the interface migrates vertically during glacial and interglacial stages. If a precursor limestone was so altered, then a similar isotopic covariance in dolomite would only be expected to be preserved under conditions wherein a low water/rock ratio is present during dolomitization. Under these conditions, the primary source for magnesium would be that supplied through the dissolution of VHMC and other high-magnesium phases. The second trend, with only a small decrease in $\delta^{18}O$ values relative to a marine dolomite, is characterized by a $\sum CO_2$ pool sourced from extensive AOM and/or sulphate reduction (Humphrey, 2000). Most mixing-zone dolomites plot in an arc between these the two end member trends (Fig. 8). The preponderance of positive $\delta^{18}O$ values suggests that such dolomites formed predominantly toward the more saline end member of a mixing zone (Fig. 8).

Analyses of $\delta^{18}O$ and clumped isotope (Δ_{47}) values in Pleistocene to Cretaceous-aged dolomite in a core in Andros Island by Winkelstern & Lohmann (2016), indicate that dolomite continues to exchange oxygen isotopes with pore fluids at burial depths in excess of 1 km. Ryb & Eiler (2018) made similar observations in a dataset of Cenozoic through Palaeozoic-aged dolomites, finding a relationship with increased age and increased equilibration at higher temperatures and more positive fluid $\delta^{18}O$ values. These

observations suggest that primary dolomite $\delta^{18}O$ values, which had previously been expected to reflect the fluid from which the mineral initially formed, should not necessarily be preserved during burial. Because of this, in order to successfully fingerprint dolomite without the potential bias of later-stage recrystallization expected from using either Δ_{47} and/or $\delta^{18}O$, the identification of the conditions in which dolomite forms must rely on the informed application of multiple isotopic systematics capable of constraining rock versus fluid buffering systems (e.g. Ahm *et al.*, 2018; Murray *et al.,* 2021). In addition, newer understanding of rock buffering of porewater composition, especially in the zone marked by dissolution of aragonite and VHMC, such as in the phreatic meteoric zone, could also bias the stable isotopic signal (Banner & Hanson, 1990; Higgins *et al.*, 2018). These, as well as the findings of Swart & Oehlert (2018) weaken the applicability of $\delta^{18}O$ alone as a clearly indicative proxy for mixing-zone alteration.

The broad range of $\delta^{13}C$ values in Fig. 8 indicates several carbon sources, including overlapping C isotope signatures resulting from multiple cycles of multi-step OM respiration processes ranging from aerobic oxidation to methanotrophy (Table 2; Charette & Sholkovitz, 2002; Brankovits *et al.*, 2017; Calderón-Gutiérrez *et al.*, 2018). The application of other isotopic proxies that are sensitive to changes in the availability of electron acceptors (for example, sulphate) could provide valuable constraint on the role of these microbial behaviours in early dolomite formation. Across the Bahamas mixing zone, for example, a strong sulphur isotope gradient can be observed, indicating significant sulphate reduction in the seawater/freshwater interface (Bottrell *et al.*, 1991). A more extended use of the isotopic composition of carbonate associated sulphate (CAS) can shed an additional light onto mixing-zone diagenesis. This latter proxy has been applied to great effect in constraining conditions during the early diagenetic history of marine sediments (Rennie & Turchyn, 2014; Present *et al.*, 2015; Murray *et al.,* 2021), and recently to the analysis of diagenetic porewaters in the Permian carbonates of the Guadalupian Mountains (Present *et al.*, 2019). Iron isotope systematics provide another redox sensitive proxy exhibiting a non-conservative behaviour across mixing zones (Rouxel *et al.*, 2008). Analysis of CAS, trace-metal enrichment factors (for example, Re, Ni and Mo) and other metal isotope systems (for example, $\delta^{238}U$ and $\delta^{98}Mo$) in suspected mixing-zone dolomite would also help in directly interrogating those dolomites for the redox state under which they formed.

The trace element and isotopic signatures of dolomite are affected by the water–rock interactions within the mixing zone. These interactions induce changes in the chemical composition of the groundwater, and in the porosity, permeability and mineralogical composition of the coastal aquifers (Wicks *et al.*, 1995; Zhao *et al.*, 2020). With respect to C and O isotopes, a low water–-rock ratio, such as might occur in a microenvironment characterized by replacement of the precursor, will result in a muting of both the $\delta^{18}O$ and $\delta^{13}C$ values of mixing-zone fluids (Fig. 8). There are, however, multiple issues involved in properly inferring water/rock ratios. These issues are also reflected by the difficulties in interpreting solution chemistries from dolomite Sr concentrations. Published values for the Sr partitioning coefficient between water and dolomite range from 0.012 (Vahrenkamp & Swart, 1990) to 0.07 (Behrens & Land, 1972), with other values in between from multiple studies (Katz *et al.*, 1972; Katz & Matthews, 1977; Baker *et al.*, 1982; Baker & Burns, 1985; Banner, 1995). This variability results in a Sr content that may range from 50 to 600 ppm for a near-stoichiometric dolomite formed from normal seawater, a range that nearly covers the entire observed Sr values observed in presumably mixing-zone dolomites (Budd, 1997). Nevertheless, Budd (1997) suggested that low-Sr dolomites (<300 ppm) are likely to be derived from unmodified seawater, whereas high-Sr dolomite (>750 ppm) likely points to a fluid with a relatively high Sr/Ca ratio derived from the dissolution of aragonite, which would point to a more diffusively limited system. Such a closed system would allow for the accumulation of Sr in the pore fluid and increase the Sr/Ca ratio of the mineral.

New developments using Ca and Mg isotopes (Higgins *et al.*, 2018) offer a new and more effective way to constrain fluid buffered versus rock buffered systems, offering insight into the physical processes present during dolomitization. Calcium isotopes, for example, when coupled with clumped isotope analyses, have been demonstrated to be a sensitive recorder of fluid advection rate (Staudigel *et al.*, 2021), this approach was effective due to the insensitivity of clumped isotopes to relative effects of rock buffering and

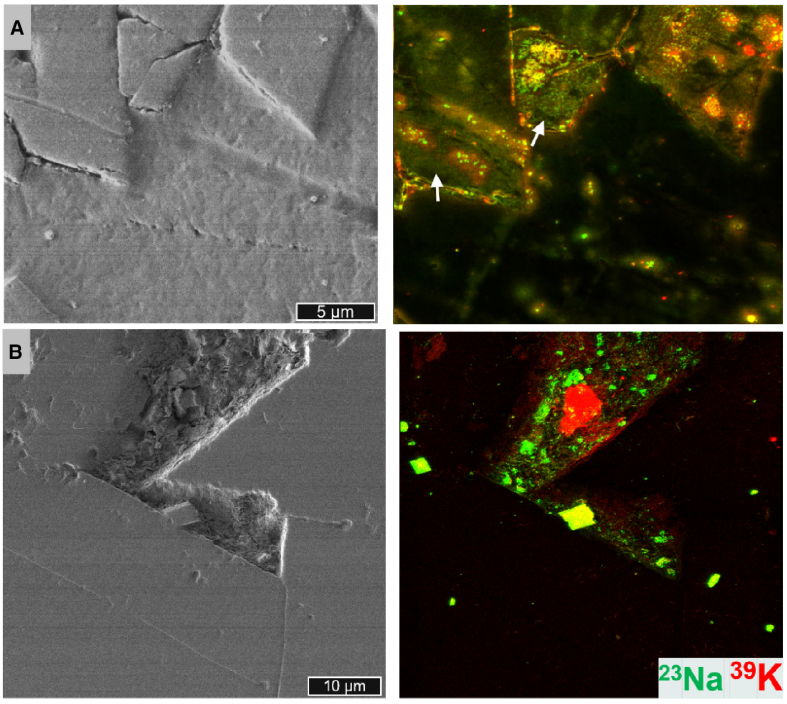

Fig. 9. Secondary ion mass spectrometry (SIMS) imaging on a He ion microscope (HIM–SIMS). This emerging technique permits petrographic analytics at the nanoscale and can also discriminate for isotopes. The analytical areas are shown in secondary electron microphotographs (left), and their corresponding elemental maps (right) are composite Na + K. (A) Fine crystalline euhedral dolomite cements from the Oligocene Suwannee Formation in the Upper Floridian aquifer. Note the presence of numerous Na + K micro-inclusions in crystals lacking these elements, likely indicative of a diagenetic chapter under the influence of more saline groundwaters that followed an earlier stage of dolomite growth in equilibrium with a fluid with low levels of these anions. Within the overgrowths, numerous nanoscale Na hotspots oriented with the *a*-axis (arrows) are interpreted to represent lattice substitution, indicative of precipitation under saline conditions. (B) Blocky dolomite cement from the Mio-Pleistocene Seroe Domi Formation in Bonaire. The partially corroded rhombs display no intracrystalline Na + K. The samples, however, contain punctual matrix accumulations of these cations. This latter feature might (or might not; Laya, *et al.*, 2021) be consistent with a downward hypersaline flux interpreted by Lucia & Major (1994).

the far higher sensitivity of calcium to the same variable. The coupled behaviour of Ca, Mg and other isotope systematics was explored in a numerical model published by Ahm *et al.* (2018) that illustrated that δ^{26}Mg and δ^{44}Ca provide ideally sensitive proxies to estimate the water/rock ratio during dolomite formation. Increase in δ^{26}Mg and δ^{44}Ca relative to an expected baseline of marine-associated values would point to a closed system. With δ^{26}Mg changing predominantly as a result of dolomite/VHMC formation, and Ca being incorporated into all carbonate phases, significant changes in δ^{26}Mg not matched with δ^{44}Ca would imply a more efficient incorporation of Mg into the solid phase products of a given diagenetic zone. Multi-proxy approaches, such as those published for Neogene Bahamian sediments (Higgins *et al.*, 2018; Murray *et al.,* 2021) and Devonian dolomite in the Williston sub-basin, within the Western Canada Sedimentary Basin (Nadeau *et al.*, 2019), therefore have the distinct advantage of being based on proxies more resistant to alteration during later stages of diagenesis. At present, little to no δ^{26}Mg and δ^{44}Ca studies of likely freshwater–seawater mixing zones or calcareous aquifers exist. A recent multi-proxy study based on a limited, yet illustrative, dataset suggests that Ca, Mg isotope values of meteorically altered, marine dolomites reflect some degree of fluid-buffered diagenetic overprint that can be constrained by the correlation of δ^{26}Mg and δ^{18}O values with δ^{44}Ca, while the corresponding δ^{13}C values and cation order inform

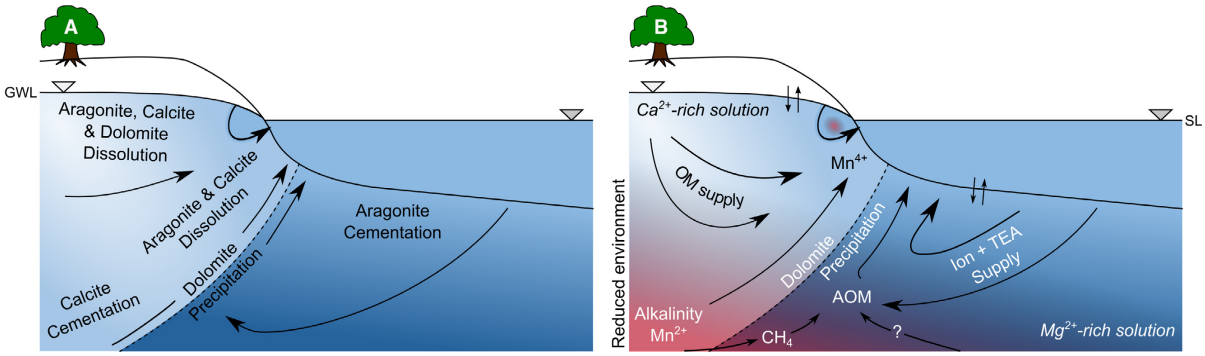

Fig. 10. Conceptual models of mixing-zone dolomitization in a coastal unconfined aquifer. (A) The traditional mixing-zone dolomitization model (Hanshaw *et al.*, 1971; Badiozamani, 1973; Land, 1973), where calcite dissolution and dolomite accumulation is controlled and dictated by differential saturation states of carbonate minerals. (B) The proposed update to the model that also incorporates the variation in alkalinity, terminal electron acceptors (TEA) and redox potential (Eh) of the system, with the red gradient illustrating the redox gradient. This is a simplified model because there are multiple elements within this system (for example, iron re-oxidation and recycling) that are yet to be fully explored with respect to dolomitization. Note that the traditional model and the proposed update is not necessarily contradictory but complementary.

on crystallization pathways (Riechelmann *et al.*, 2020). A chemostratigraphic application of these combined isotope systems, ideally with petrographic control, to mixing-zone settings could prove highly informative if evaluated with respect to the meaning of their covariant mineral assemblages and water/rock ratios.

Emerging methods and techniques such as clumped isotopes could also be applied to younger mixing-zone dolomites (i.e. examples where enough dolomite can be concentrated with minimal concern about mixing phases), which would yield palaeotemperatures of formation and allow constraining equilibrium pore fluid $\delta^{18}O$ values. The latter would shed light on the salinity regime which generated these dolomites. Detailed $\delta^{18}O$ and $\delta^{13}C$ analysis of zoned dolomite crystals using secondary ion mass spectrometry (SIMS) (Śliwiński *et al.*, 2016a,b) would also be helpful to elucidate the presence/absence of the highly variable isotopic signals predicted by temporal and spatial variation in the amount of mixing and biogeochemical reactions that affect the carbon system. Interestingly, this technique is also prospective for the evaluation of the intracrystalline distribution of salinity indicator elements, such as sodium and potassium (Fig. 9). High resolution analyses of these elements can be combined with *in situ* $\delta^{18}O$ microanalyses of zoned dolomite for compositional estimations of the dolomitizing fluid in the mixing zone. Application of any or a combination of these emerging characterization techniques to hypothetical examples of mixing-zone dolomite represents a research opportunity that could illuminate further aspects of mixing-zone diagenesis.

CONCLUDING REMARKS

1 The arguments once declaring the classical mixing-zone dolomitization model as a failed hypothesis are shown to be scientifically unsatisfactory. The original conception of the model, however, did not account for the biogeochemical intricacy of the carbonate system. A more sophisticated alternative model was therefore required.

2 This updated conceptual and mechanistic perspective of dolomitization in mixed-source coastal aquifers (Fig. 10) encompasses high frequency changes in relative sea-level and climate variations as modulators of the redox structure of mixing zones. Concurrent with changes in the redox potentials, the upper part of mixing zones can recurrently become the locus of reoxidation of the reduced species. Recycling of these energy sources involves the long-term activity and interlinked dynamics of diverse microbial communities thriving best within the redoxcline of coastal mixing zones, as suggested by the currently available microbiome and

isotope analyses of the Yucatan and Florida examples.

3 The redox structure in the coastal mixing zone is not static and shifts with changes in relative sea level, and as a response of quasi-periodic climatic fluctuations between wet and dry periods. Concomitant changes in porewater hydrochemistry can allow for a downstream reaction (for example, oxidation) to shift to the prior position of the corresponding upstream reaction (for example, reduction). As a result of these redox oscillations, notably during glacial periods, the biogeochemical reaction front in the mixing zone can sweep across an entire shelf. Cycles of enhanced selective dissolution affecting primarily very high-Mg calcite (VHMC) and aragonitic constituents, reprecipitation of precursors as dolomite, and cementation by the latter in the deep phreatic saline zone, where Mg^{2+} ion availability is increased, and the abundance of terminal electron acceptors (TEA) also allows for reducing conditions to develop. The mechanism can become particularly efficient when the moveable diagenetic front passes repeatedly through shallowly buried facies containing an abundance of early diagenetic authigenic VHMC ± poorly ordered Ca-dolomite.

4 The genomic and isotopic evidence, when combined with the range of recorded variations in ΣCO_2, pCO_2, alkalinity and pH ranges, indicates that biogeochemistry regulates key parameters of the inorganic carbon system within mixing zones. Also, important is that the organic carbon turnover within the mixing zone appears to be exerted by metabolic functions like those that have been thought instrumental for shallow marine, near-surface dolomite precipitation environments. These include, among others, N, Fe, Mn and S-based heterotrophic pathways, as well as chemoautotrophy and methanotrophy.

5 The petrographic and geochemical observations of dolomitic successions interpreted to be the product of mixing-zone diagenesis were re-evaluated. This reassessment supports coastal mixing zones as viable diagenetic domains for the formation of dolomite both as neomorphic phases that replace early aragonite and VHMC precursors, and as newly formed cements often exhibiting a heterogenous elemental composition (Mg/Ca, Mn, Fe and Na) at the crystal scale. These features result not just from relative solubility differences between carbonate minerals but is also reflective of complex redox fluctuations interlinked to the long-term C cycle in coastal aquifers.

6 The empirical geochemical evidence supports an active elemental recycling processes in Neogene coastal aquifers, but the role of manganese, zinc, intermediate sulphur and nitrogen species as drivers of dolomitization are far from being fully understood, nor is their fingerprint in ancient deposits exhibiting a mixing-zone diagenetic imprint. Combined traditional and emerging geochemical proxies including high-resolution imaging techniques and more extended use and integration of of Δ_{47}, Mg, Ca and Fe isotope systematics, together with more detailed analyses of the carbonate associated sulphur isotopes, and redox sensitive elemental concentration data provide opportunities to truly evaluate a mixing-zone origin of Neogene and by extrapolation more ancient dolomites. This effort will also shed light on the long-term dynamics of subsurface communities in diagenetic mixing-zone systems.

ACKNOWLEDGEMENTS

The authors are thankful to Adrian Immenhauser, two anonymous reviewers at *Sedimentology* and Associate Editor Eric Hiatt for constructive criticism, insightful reviews, suggestions and editorial input that substantially improved the manuscript. DAP acknowledges partial support by Czech Geological Survey and the Czech Science Foundation (19-15096Y). DAP also thanks Peter Gnauck, Carl Zeiss Microscopy GmbH, and J. Nicolas Audinot, Luxembourg Institute of Science and Technology (LIST), for allocating proof-of-concept analyses in the HIM instrument coupled with a SIMS system being developed at LIST. OMB was partially supported by ISF grant No. 2208/15 based on research agreements between the Israeli Science Foundation and the National Science Foundation of China in conjunction to NSFC grant No. 41561144002 and is currently supported by Marie Skłodowska Curie fellowship 101003394 (RhodoMalta). DAB thanks H. L Vacher for introducing him to the rocks of the Floridan Aquifer, and acknowledges past students Brent Johnson, Nick Loizeaux and Stephanie Gaswirth for their insight on topics discussed in this contribution. Samples from the Neogene dolomites of the Floridan aquifer and Curaçao/Bonaire were collected with the support to DAB from the Petroleum Research Fund and the industrial associates of the

Analysis of Variability in Dolomites (AVID) consortium, respectively. The authors have no conflict of interest to report.

REFERENCES

Ahm, A.S.C., **Bjerrum, C.J.**, **Blättler, C.L.**, **Swart, P.K.** and **Higgins, J.A.** (2018) Quantifying early marine diagenesis in shallow-water carbonate sediments. *Geochim. Cosmochim. Acta*, **236**, 140–159.

Allan, J.R. and **Matthews, R.K.** (1982) Isotope signatures associated with early meteoric diagenesis. *Sedimentology*, **29**, 797–817.

Arvidson, R.S. and **Mackenzie, F.T.** (1997) Tentative kinetic model for dolomite precipitation rate and its application to dolomite distribution. *Aquat. Geochem.*, **2**, 273–298.

Back, W. and **Hanshaw, B.B.** (1970) Comparison of chemical hydrogeology of the carbonate peninsulas of Florida and Yucatan. *J. Hydrol.*, **10**, 330–368.

Back, W., **Hanshaw, B.B.**, **Herman, J.S.** and **Van Driel, J.N.** (1986) Differential dissolution of a Pleistocene reef in the ground-water mixing zone of coastal Yucatan, Mexico. *Geology*, **14**, 137.

Badiozamani, K. (1973) The Dorag dolomitization model - Application to the Middle Ordovician of Wisconsin. *J. Sediment. Res.*, **43**, 965–984.

Baker, P.A. and **Burns, S.J.** (1985) Occurrence and formation of dolomite in organic-rich continental margin sediments. *Am. Assoc. Pet. Geol. Bull.*, **69**, 1917–1930.

Baker, P.A., **Gieskes, J.M.** and **Elderfield, H.** (1982) Diagenesis of carbonates in deep-sea sediments–Evidence from Sr/Ca ratios and interstitial sissolved Sr2+ data. *J. Sediment. Res.*, **52**, 71–82.

Banner, J.L. (1995) Application of the trace element and isotope geochemistry of strontium to studies of carbonate diagenesis. *Sedimentology*, **42**, 805–824.

Banner, J.L. and **Hanson, G.N.** (1990) Calculation of simultaneous isotopic and trace element variations during water-rock interaction with applications to carbonate diagenesis. *Geochim. Cosmochim. Acta*, **54**, 3123–3137.

Barnaby, R.J. and **Rimstidt, J.D.** (1989) Redox conditions of calcite cementation interpreted from Mn and Fe contents of authigenic calcites. *Geol. Soc. Am. Bull.*, **101**, 795–804.

Beal, E.J., **House, C.H.** and **Orphan, V.J.** (2009) Manganese- and iron-dependent marine methane oxidation. *Science*, **325**, 184–187.

Befus, K.M., **Kroeger, K.D.**, **Smith, C.G.** and **Swarzenski, P.W.** (2017) The magnitude and origin of groundwater discharge to Eastern U.S. and Gulf of Mexico Coastal Waters. *Geophys. Res. Lett.*, **44**, 10396–10406.

Behrens, E.W. and **Land, L.S.** (1972) Subtidal Holocene Dolomite, Baffin Bay, Texas. *J. Sediment. Res.*, **42**, 155–161.

Beulig, F., **Røy, H.**, **Glombitza, C.** and **Jørgensen, B.B.** (2018) Control on rate and pathway of anaerobic organic carbon degradation in the seabed. *Proc. Natl. Acad. Sci.*, **115**, 367–372.

Boehm, A.B., **Paytan, A.**, **Shellenbarger, G.G.** and **Davis, K.A.** (2006) Composition and flux of groundwater from a California beach aquifer: Implications for nutrient supply to the surf zone. *Cont. Shelf Res.*, **26**, 269–282.

Bontognali, T.R.R., **Vasconcelos, C.**, **Warthmann, R.J.**, **Bernasconi, S.M.**, **Dupraz, C.**, **Strohmenger, C.J.** and **McKenzie, J.A.** (2010) Dolomite formation within microbial mats in the coastal sabkha of Abu Dhabi (United Arab Emirates). *Sedimentology*, **57**, 824–844.

Böttcher, M.E. and **Thamdrup, B.** (2001) Oxygen and sulfur isotope fractionation during anaerobic bacterial disporportioanation of elemental sulfur. *Geochim. Cosmochim. Acta*, **65**, 1601–1609.

Bottrell, S.H., **Smart, P.L.**, **Whitaker, F.** and **Raiswell, R.** (1991) Geochemistry and isotope systematics of sulphur in the mixing zone of Bahamian blue holes. *Appl. Geochem.*, **6**, 97–103.

Boudreau, B.P. and **Ruddick, B.R.** (1991) On a reactive continuum representation of organic matter diagenesis. *Am. J. Sci.*, **291**, 507–538.

Brankovits, D., **Pohlman, J.W.**, **Niemann, H.**, **Leigh, M.B.**, **Leewis, M.C.**, **Becker, K.W.**, **Iliffe, T.M.**, **Alvarez, F.**, **Lehmann, M.F.** and **Phillips, B.** (2017) Methane- and dissolved organic carbon-fueled microbial loop supports a tropical subterranean estuary ecosystem. *Nat. Commun.*, **8**, 1835.

Budd, D.A. (1997) Cenozoic dolomites of carbonate islands: their attributes and origin. *Earth-Sci. Rev.*, **42**(1-2), 1–47.

Budd, D.A., **Hammes, U.** and **Ward, W.B.** (2000) Cathodoluminescence in Calcite Cements: New Insights on Pb and Zn Sensitizing, Mn Activation, and Fe Quenching at Low Trace-Element Concentrations. *J. Sediment. Res.*, **70**, 217–226.

Budd, D.A. and **Mathias, W.D.** (2015) Formation of lateral patterns in rock properties by dolomitization: Evidence from a miocene reaction front (Bonaire, Netherlands Antilles). *J. Sediment. Res.*, **85**, 1082–1101.

Calderón-Gutiérrez, F., **Sánchez-Ortiz, C.A.** and **Huato-Soberanis, L.** (2018) Ecological patterns in anchialine caves. *PLoS One*, **13**, e0202909.

Cander, H.S. (1992) Dolomitization and water-rock interaction in the middle Eocene Avon Park Formation, Floridan Aquifer. 6280–6280. Dolomitization and water - rock interaction in the middle Eocene Avon Park Formation, Floridan aquifer, Ph.D. Dissertation, The University of Texas at Austin. Austin, Texas, 172 p.

Cander, H.S. (1994) An example of mixing-zone dolomite, Middle Eocene Avon Park Formation, Floridan Aquifer System. *J. Sediment. Res.*, **64A**, 615–629.

Canfield, D.E., **Thamdrup, B.** and **Fleischer, S.** (1998) Isotope fractionation and sulfur metabolism by pure and enrichment cultures of elemental sulfur-disproportionating bacteria. *Limnol. Oceanogr.*, **43**, 253–264.

Canul-Macario, C., **González-Herrera, R.**, **Sánchez-Pinto, I.** and **Graniel-Castro, E.** (2019) Contribution to the evaluation of solute transport properties in a karstic aquifer (Yucatan, Mexico). *Hydrogeol. J.*, **27**, 1683–1691.

Chafetz, H.S., **Imerito-Tetzlaff, A.A.** and **Zhang, J.** (1999) Stable-isotope and elemental trends in pleistocene sabkha dolomites: Descending meteoric water vs. sulfate reduction. *J. Sediment. Res.*, **69**, 256–266.

Chafetz, H. and **Rush, P.F.** (1994) Diagenetically altered sabkha-type Pleistocene dolomite from the Arabian Gulf. *Sedimentology*, **41**, 409–421.

Chapelle, F.H., **McMahon, P.B.**, **Dubrovsky, N.M.**, **Fujii, R.F.**, **Oaksford, E.T.** and **Vroblesky, D.A.** (1995) Deducing the distribution of terminal electron-accepting processes in hydrologically diverse groundwater systems. *Water Resour. Res.*, **31**, 359–371.

Charette, M.A. (2007) Hydrologic forcing of submarine groundwater discharge: Insight from a seasonal study of

radium isotopes in a groundwater-dominated salt marsh estuary. *Limnol. Oceanogr.*, **52**, 230–239.

Charette, M.A. and **Sholkovitz, E.R.** (2002) Oxidative precipitation of groundwater-derived ferrous iron in the subterranean estuary of a coastal bay. *Geophys. Res. Lett.*, **29**, 85-1-85–4.

Choquette, P.W. and **Hiatt, E.E.** (2008) Shallow-burial dolomite cement: a major component of many ancient sucrosic dolomites. *Sedimentology*, **55**, 423–460.

Choquette, P.W. and **Steinen, R.P.** (1980) Mississippian non-supratidal dolomite, Ste. Genevieve Limestone, Illinois Basin: evidence for mixed-water dolomitization. In *Concepts and Models of Dolomitization* (Eds Zenger, D.H., Dunham, J.B. and Ethington, R.L.), *SEPM Society for Sedimentary Geology*, **28**, 163–196.

Coniglio, M., **James, N.P.** and **Aissaoui, D.M.** (1988) Dolomitization of Miocene Carbonates, Gulf of Suez, Egypt. *SEPM J. Sediment. Res.*, **58**, 100–119.

Csoma, A.E., **Goldstein, R.H.**, **Mindszenty, A.** and **Simone, L.** (2004) Diagenetic salinity cycles and sea level along a major unconformity, Monte Composauro, Italy. *J. Sediment. Res.*, **74**, 889–903.

Davis, M. and **Garey, J.** (2018) Microbial function and hydrochemistry within a stratified anchialine sinkhole: A window into coastal aquifer interactions. *Water*, **10**, 972.

Daye, M., **Higgins, J.** and **Bosak, T.** (2019) Formation of ordered dolomite in anaerobic photosynthetic biofilms. *Geology*, **47**, 1–4.

De Sieyes, N.R., **Yamahara, K.M.**, **Layton, B.A.**, **Joyce, E.H.** and **Boehm, A.B.** (2008) Submarine discharge of nutrient-enriched fresh groundwater at Stinson Beach. *Limnol. Oceanogr.*, **53**, 1434–1445.

Dickson, A.G. (2010) The carbon dioxide system in seawater: equilibrium chemistry and measurements. In: *Guide to best practices for ocean acidification research and data reporting* (Eds Riebesell, U., Fabry, V.J., Hansson, L. and Gattuso, J.-P.), pp. 17–40.Publications Office of the European Union, Luxembourg.

Edwards, K.J., **Becker, K.** and **Colwell, F.** (2012) The Deep, Dark Energy Biosphere: Intraterrestrial Life on Earth. *Annu. Rev. Earth Planet. Sci.*, **40**, 551–568.

Folk, R.L. and **Land, L.S.** (1975) Mg/Ca ratio and salinity: Two Controls over crystallization of dolomite. *Am. Assoc. Pet. Geol. Bull.*, **59**, 60–68.

Fouke, B.W. (1993) *Chronostratigraphy and dolomitization of the Seroe Domi Formation, Curaçao, Netherlands Antilles*. Unpublished PhD Dissertation. University of New York at Stony Brook, Stony Brook, NY.

Fouke, B.W. (1994) *Deposition, diagenesis and dolomitization of Neogene Seroe Domi Formation coral reef limestones on Curaçao, Netherlands Antilles*. Publications Foundation for scientific research in the Caribbean region, Amsterdam, 182 pp.

Fouke, B.W., **Beets, C.J.**, **Meyers, W.J.**, **Hanson, G.N.**, **Brook, S.**, **Melillo, A.J.** and **Orleans, N.** (1996) 87Sr/86Sr chronostratigraphy and dolomitization history of the Seroe Domi Formation, Curacao (Netherlands Antilles). *Facies*, **35**, 293–320.

Froelich, P.N., **Klinkhammer, G.P.**, **Bender, M.L.**, **Luedtke, N.A.**, **Heath, G.R.**, **Cullen, D.**, **Dauphin, P.**, **Hammond, D.**, **Hartman, B.** and **Maynard, V.** (1979) Early oxidation of organic matter in pelagic sediments of the eastern equatorial Atlantic: suboxic diagenesis. *Geochim. Cosmochim. Acta*, **43**, 1075–1090.

Frausto, O., **Mattes, L.**, **Ilh, T.**, **Cervantes, A.** and **Giese, S.** (2008) Groundwater Quality Monitoring on Northeast Yucatan Peninsula, Mexico. Presented at 20th Salt Water Intrusion Meeting. June 23–27, 2008 Naples, Florida. http://www.falw.vu/~swim/pdf/swim20/file099-102.pdf. Retrieved 4/10/20.

Gaswirth, S.B., **Budd, D.A.** and **Lang Farmer, G.** (2007) The role and impact of freshwater–seawater mixing zones in the maturation of regional dolomite bodies within the proto Floridan Aquifer, USA. *Sedimentology*, **54**, 1065–1092.

Gebelein, C.D., **Steinen, R.P.**, **Garret, P.**, **Hoffmann, E.J.**, **Queen, J.M.** and **Plummer, L.N.** (1980) Subsurface dolomitization beneath the tidal flats of Central-West Andros Island, Bahamas. In: *Concepts and Models of Dolomitization* (Ed. Zenger, D.H., Dunham, J.B. and Ethington, R.L.), *SEPM Special publication* **28**, 31–48.

Geske, A., **Lokier, S.**, **Dietzel, M.**, **Richter, D.K.**, **Buhl, D.** and **Immenhauser, A.** (2015) Magnesium isotope composition of sabkha porewater and related (Sub-)Recent stoichiometric dolomites, Abu Dhabi (UAE). *Chem. Geol.*, **393–394**, 112–124.

Gies, H. (1975) Activation possibilities and geochemical correlations of photoluminescing carbonates, particularly calcites. *Miner. Depos.*, **10**, 216–227.

Gondwe, B.R.N., **Lerer, S.**, **Stisen, S.**, **Marín, L.**, **Rebolledo-Vieyra, M.**, **Merediz-Alonso, G.** and **Bauer-Gottwein, P.** (2010) Hydrogeology of the south-eastern Yucatan Peninsula: New insights from water level measurements, geochemistry, geophysics and remote sensing. *J. Hydrol.*, **389**, 1–17.

Gonneea, M.E., **Charette, M.A.**, **Liu, Q.**, **Herrera-Silveira, J.A.** and **Morales-Ojeda, S.M.** (2014) Trace element geochemistry of groundwater in a karst subterranean estuary (Yucatan Peninsula, Mexico). *Geochim. Cosmochim. Acta*, **132**, 31–49.

González, L.A., **Ruiz, H.M.**, **Taggart, B.E.**, **Budd, A.F.** and **Monell, V.** (1997) Geology of Isla de Mona, Puerto Rico. In: *Geology and Hydrogeology of Carbonate Islands* (Eds Vacher, H.L. and Quinn, T.M.), *Developments in Sedimentology*, **54**, 327–358.

Gregg, J.M., **Bish, D.L.**, **Kaczmarek, S.E.** and **Machel, H.G.** (2015) Mineralogy, nucleation and growth of dolomite in the laboratory and sedimentary environment: A review. *Sedimentology*, **62**, 1749–1769.

Habermann, D., **Neuser, R.D.** and **Richter, D.K.** (1996) REE-activated cathodoluminescence of calcite and dolomite: high-resolution spectrometric analysis of CL emission (HRS-CL). *Sediment. Geol.*, **101**, 1–7.

Hagens, M. and **Middelburg, J.J.** (2016) Generalised expressions for the response of pH to changes in ocean chemistry. *Geochim. Cosmochim. Acta*, **187**, 334–349.

Ham, J.D. (1972) Chemical factors that influence the availability of iron and manganese in aqueous systems. *GSA Bull.*, **83**, 443–450.

Hanshaw, B.B., **Back, W.** and **Deike, R.G.** (1971) A geochemical hypothesis for dolomitization by Ground Water. *Econ. Geol.*, **66**, 710–724.

Haque, S.E. and **Johannesson, K.H.** (2006) Concentrations and speciation of arsenic along a groundwater flow-path in the Upper Floridan aquifer, Florida, USA. *Environ. Geol.*, **50**, 219–228.

Herman, J.S., **Back, W.** and **Pomar, L.** (1985) Geochemistry of groundwater in the mixing zone along the East coast of Mallorca, Spain. In: *Karst Water Resources* (Ed.

Proceedings of the Ankara - Antalya Symposium), *IAHS Publication* **161**, 467–479.

Higgins, J.A., **Blättler, C.L.**, **Lundstrom, E.A.**, **Santiago-Ramos, D.P.**, **Akhtar, A.A.**, **Crüger Ahm, A.-S.-A.-S.**, **Bialik, O.**, **Holmden, C.**, **Bradbury, H.**, **Murray, S.T.** and **Swart, P.K.** (2018) Mineralogy, early marine diagenesis, and the chemistry of shallow-water carbonate sediments. *Geochim. Cosmochim. Acta*, **220**, 512–534.

Hulth, S., **Aller, R.C.** and **Gilbert, F.** (1999) Coupled anoxic nitrification/manganese reduction in marine sediments. *Geochim. Cosmochim. Acta*, **63**, 49–66.

Humphrey, J.D. (1988) Late Pleistocene mixing zone dolomitization, southeastern Barbados, West Indies. *Sedimentology*, **35**, 327–348.

Humphrey, J.D. (2000) New geochemical support for mixing-zone dolomitization at Golden Grove, Barbados. *J. Sediment. Res.*, **70**, 1160–1170.

Humphrey, J.D. and **Kimbell, T.N.** (1990) Sedimentology and sequence stratigraphy of upper Pleistocene carbonates of southeastern Barbardos, West Indies. *Am. Assoc. Pet. Geol. Bull.*, **74**, 1671–1684.

Humphrey, J.D. and **Quinn, T.M.** (1989) Coastal mixing zone dolomite, forward modeling, and massive dolomitization of platform-margin carbonates. *J. Sediment. Res.*, **59**, 438–454.

Humphrey, J.D. and **Radjef, E.M.** (1991) Dolomite stoichiometric variability resulting from changing aquifer conditions, Barbados, West Indies. *Sediment. Geol.*, **71**, 129–136.

James, N.P., **Bone, Y.** and **Kyser, T.K.** (1993) Shallow burial dolomitization and dedolomitization of mid-Cenozoic, cool-water, calcitic, deep-shelf limestones, southern Australia. *J. Sediment. Petrol.*, **63**, 528–538.

Jewell, T.N.M., **Karaoz, U.**, **Brodie, E.L.**, **Williams, K.H.** and **Beller, H.R.** (2016) Metatranscriptomic evidence of pervasive and diverse chemolithoautotrophy relevant to C, S, N and Fe cycling in a shallow alluvial aquifer. *ISME J.*, **10**, 2106–2117.

Jewell, T.N.M., **Karaoz, U.**, **Bill, M.**, **Chakraborty, R.**, **Brodie, E.L.**, **Williams, K.H.** and **Beller, H.R.** (2017) Metatranscriptomic analysis reveals unexpectedly diverse microbial metabolism in a biogeochemical hot spot in an alluvial aquifer. *Front. Microbiol.*, **8**. https://doi.org/10.3389/fmicb.2017.00040.

Jiang, J., **Gao, M.-R.**, **Qiu, Y.-H.**, **Wang, G.-S.**, **Liu, L.**, **Cai, G.-B.** and **Yu, S.-H.** (2011) Confined crystallization of polycrystalline high-magnesium calcite from compact Mg-ACC precursor tablets and its biological implications. *CrystEngComm*, **13**, 952–956.

Johannesson, K.H., **Chevis, D.A.**, **Burdige, D.J.**, **Cable, J.E.**, **Martin, J.B.** and **Roy, M.** (2011) Submarine groundwater discharge is an important net source of light and middle REEs to coastal waters of the Indian River Lagoon, Florida, USA. *Geochim. Cosmochim. Acta*, **75**, 825–843.

Jones, B. (1989) Syntaxial overgrowths on dolomite crystals in the Bluff Formation, Grand Cayman, British West Indies. *J. Sediment. Petrol.*, **59**, 839–847.

Jones, B. (2007) Inside-Out Dolomite. *J. Sediment. Res.*, **77**, 539–551.

Jones, I.C., **Vacher, H.L.** and **Budd, D.A.** (1993) Transport of calcium, magnesium and SO4 in the Floridan aquifer, west-central Florida: implications to cementation rates. *J. Hydrol.*, **143**, 455–480.

Kaczmarek, S.E. and **Sibley, D.F.** (2014) Direct physical evidence of dolomite recrystallization. *Sedimentology*, **61**, 1862–1882.

Katz, A. and **Matthews, A.** (1977) The dolomitization of CaCO3: an experimental study at 252–295°C. *Geochim. Cosmochim. Acta*, **41**, 297–308.

Katz, A., **Sass, E.**, **Starinsky, A.** and **Holland, H.** (1972) Strontium behavior in the aragonite-calcite transformation: An experimental study at 40–98°C. *Geochim. Cosmochim. Acta*, **36**, 481–496.

Katz, B.G. (1992) *Hydrochemistry of the Upper Floridan Aquifer, Florida*. Report 91-4196. U.S. Geological Survey Water-Resources Investigations, Tallahassee, FL, 43 pp.

Kell-Duivestein, I.J., **Baldermann, A.**, **Mavromatis, V.** and **Dietzel, M.** (2019) Controls of temperature, alkalinity and calcium carbonate reactant on the evolution of dolomite and magnesite stoichiometry and dolomite cation ordering degree - An experimental approach. *Chem. Geol.*, **529**, 119292.

Kimbell, T.N. (1993) *Sedimentology and Diagenesis of Late Pleistocene Fore-reef Calcarenites, Barbados, West Indies: A Geochemical and Petrographic Investigation of Mixing Zone Diagenesis*. Unpublished PhD Dissertation. University of Texas, Dallas, TX.

Konhauser, K. (2007) *Introduction to Geomicrobiology*. Blackwell Pub, Oxford, 440 pp.

Krężel, A. and **Maret, W.** (2016) The biological inorganic chemistry of zinc ions. *Arch. Biochem. Biophys.*, **611**, 3–19.

Kroeger, K.D. and **Charette, M.A.** (2008) Nitrogen biogeochemistry of submarine groundwater discharge. *Limnol. Oceanogr.*, **53**, 1025–1039.

Kyser, T.K., **James, N.P.** and **Bone, Y.** (2002) Shallow Burial dolomitization and dedolomitization of cenozoic cool-water limestones, Southern Australia: Geochemistry and origin. *J. Sediment. Res.*, **72**, 146–157.

Land, L.S. (1973) Contemporaneous dolomitization of Middle Pleistocene reefs by meteoric water, North Jamaica. *Bull. Mar. Sci.*, **23**, 64–92.

Land, L.S. (1985) The origin of massive dolomite. *J. Geol. Educ.*, **33**, 112–125.

Land, L.S. (1991) Dolomitization of the Hope Gate Formation (North Jamaica) by seawater; reassessment of mixing-zone dolomite. In: *Stable Isotope Geochemistry: A Tribute to Samuel Epstein* (Eds Taylor, H.P., O'Neil, J.R. and Kaplan, I.R.), *Geochemical Society, Spec. Publ.*, **3**, 121–133.

Land, L. (1998) Failure to precipitate dolomite at 25° C from dilute solution despite 1000-fold oversaturation after 32 years. *Aquat. Geochemistry*, **4**, 361–368.

LaRowe, D.E. and **Amend, J.P.** (2015) Power limits for microbial life. *Front. Microbiol.*, **6**. https://doi.org/10.3389/fmicb.2015.00718.

Lasemi, Z., **Boardman, M.R.** and **Sandberg, P.A.** (1989) Cement origin of supratidal dolomite. *J. Sediment. Res.*, **59**, 249–257.

Laya, J.C., **Teoh, C.P.**, **Whitaker, F.**, **Manche, C.**, **Kaczmarek, S.**, **Tucker, M.**, **Gabellone, T.** and **Hasiuk, F.** (2021) Dolomitization of a Miocene-Pliocene progradational carbonate platform by mesohaline brines: re-examination the reflux model on Bonaire Island. *Mar. Pet. Geol.*, 104895.

Lee, K. and **Millero, F.J.** (1995) Thermodynamic studies of the carbonate system in seawater. *Deep Sea Res. Part I Oceanogr. Res. Pap.*, **42**, 2035–2061.

Li, W., **Bialik, O.M.**, **Wang, X.**, **Yang, T.**, **Hu, Z.**, **Huang, Q.**, **Zhao, S.** and **Waldmann, N.D.** (2019a) Effects of early diagenesis on Mg isotopes in dolomite: The roles of Mn (IV)-reduction and recrystallization. *Geochim. Cosmochim. Acta*, **250**, 1–17.

Li, Y., **Wang, X.**, **Li, Y.**, **Duan, J.**, **Jia, H.**, **Ding, H.**, **Lu, A.**, **Wang, C.**, **Nie, Y.** and **Wu, X.** (2019b) Coupled anaerobic and aerobic microbial processes for Mn-carbonate precipitation: A realistic model of inorganic carbon pool formation. *Geochim. Cosmochim. Acta.*, **256**, 49–65.

Lohmann, K.C. (1988) Geochemical patterns of meteoric diagenetic systems and their application to studies of Paleokarst. In: *Paleokarst* (Eds James, N.P. and Choquette, P.W.), pp. 58–80.Springer, New York, NY.

Lovley, D.R. and **Chapelle, F.H.** (1995) Deep subsurface microbial processes. *Rev. Geophys.*, **33**, 365–381.

Loyd, S.J., **Berelson, W.M.**, **Lyons, T.W.**, **Hammond, D.E.** and **Corsetti, F.A.** (2012) Constraining pathways of microbial mediation for carbonate concretions of the Miocene Monterey Formation using carbonate-associated sulfate. *Geochim. Cosmochim. Acta*, **78**, 77–98.

Lucia, F.J. and **Major, R.P.** (1994) Porosity evolution through hypersaline reflux dolomitization. In: *Dolomites: A volume in honour of Dolomieu* (Eds Purser, B., Tucker, M. and Zenger, D.), pp. 325–341.Blackwell Publishing Ltd., Oxford.

Machel, H.G. (1985) Cathodoluminescence in calcite and dolomite and its chemical interpretation. *Geosci. Canada*, **12**, 139–147.

Machel, H.G. (2004) Concepts and models of dolomitization: a critical reappraisal. In: *The Geometry and Petrogenesis of Dolomite Hydrocarbon Reservoirs* (Eds Braithwaite, C., Rizzzi, G. and Darke, G.), *Geological Society. London, Special Publications*, **235**, 7–63.

Machel, H.G., **Mason, R.A.**, **Mariano, A.N.** and **Mucci, A.** (1991) Causes and emission of luminescence in calcite and dolomite. In: *Luminescence Microscopy and Spectroscopy: Qualitative and Quantitative Applications* (Ed. Barker, C.E., Burruss, R.C., Kopp, O.C., Machel, H.G., Marshall, D.J., Wright, P. and Colbum, H.Y.), *SEPM Short Course Notes*, **25**, 37–57.

Machel, H.-G. and **Mountjoy, E.W.** (1986) Chemistry and environments of dolomitization — A reappraisal. *Earth Sci. Rev.*, **23**, 175–222.

Mackenzie, F.T. and **Andersson, A.J.** (2013) The marine carbon system and ocean acidification during Phanerozoic time. *Geochem. Perspect.*, **2**, 1–176.

Magaritz, M., **Goldenberg, L.**, **Kafri, U.** and **Arad, A.** (1980) Dolomite formation in the seawater–freshwater interface. *Nature*, **287**, 622–624.

Manche, C.J. and **Kaczmarek, S.E.** (2019) Evaluating reflux dolomitization using a novel high-resolution record of dolomite stoichiometry: A case study from the Cretaceous of central Texas, USA. *Geology*, **47**, 586–590.

Matsuda, H., **Tsuji, Y.**, **Honda, N.** and **Saotome, J.** (1995) Early Diagenesis of Pleistocene Carbonates from a Hydrogeochemical Point of View, Irabu Island, Ryukyu Islands: Porosity Changes Related to Early Carbonate Diagenesis. In: *AAPG Memoir 63: Unconformities and Porosity in Carbonate Strata* (Eds Budd, D.A. and Saller, P.M.), *American Association of Petroleum Geologists*, **63**, 313.

Matthews, R.K. and **Frohlich, C.** (1987) Forward modeling of bank-margin carbonate diagenesis. *Geology*, **15**, 673.

Mazzullo, S.J., **Reid, A.M.** and **Gregg, J.M.** (1987) Dolomitization of Holocene Mg-calcite supratidal deposits, Ambergris Cay. *Belize. Geol. Soc. Am. Bull.*, **98**, 224.

McAllister, S.M., **Barnett, J.M.**, **Heiss, J.W.**, **Findlay, A.J.**, **MacDonald, D.J.**, **Dow, C.L.**, **Luther, G.W.**, **Michael, H.A.** and **Chan, C.S.** (2015) Dynamic hydrologic and biogeochemical processes drive microbially enhanced iron and sulfur cycling within the intertidal mixing zone of a beach aquifer. *Limnol. Oceanogr.*, **60**, 329–345.

McMahon, P. (2001) Aquifer/aquitard interfaces: mixing zones that enhance biogeochemical reactions. *Hydrogeol. J.*, **9**, 34–43.

Melim, L.A., **Swart, P.K.** and **Eberli, G.P.** (2004) Mixing-zone diagenesis in the subsurface of Florida and the Bahamas. *J. Sediment. Res.*, **74**, 904–913.

Michael, H.A., **Mulligan, A.E.** and **Harvey, C.F.** (2005) Seasonal oscillations in water exchange between aquifers and the coastal ocean. *Nature*, **436**, 1145–1148.

Middelburg, J.J. (2019) *Marine Carbon Biogeochemistry. A Primer for Earth System Scientists*. Springer International Publishing, Cham, Switzerland, 118 pp.

Millero, F.J. (1995) Thermodynamics of the carbon dioxide system in the oceans. *Geochim. Cosmochim. Acta*, **59**, 661–677.

Mitchell, J.T., **Land, L.S.** and **Miser, D.E.** (1987) Modern marine dolomite cement in a north Jamaican fringing reef. *Geology*, **15**, 557–560.

Mucci, A. (1983) The solubility of calcite and aragonite in seawater at various salinities, temperatures, and one atmosphere total pressure. *Am. J. Sci.*, **283**, 780–799.

Muchez, P. and **Viaene, W.** (1994) Dolomitization caused by water circulation near the mixing zone: An example from the Lower Visof the Campine Basin (Northern Belgium). In: *Dolomites: A Volume in Honour of Dolomieu* (Eds Purser, B., Tucker, M. and Zenger, D.), pp. 155–166.Blackwell Publishing Ltd., Oxford.

Müller, I.A., **Rodriguez-Blanco, J.D.**, **Storck, J.C.**, **Do Nascimento, G.S.**, **Bontognali, T.R.R.**, **Vasconcelos, C.**, **Benning, L.G.** and **Bernasconi, S.M.** (2019) Calibration of the oxygen and clumped isotope thermometers for (proto-)dolomite based on synthetic and natural carbonates. *Chem. Geol.*, **525**, 1–17.

Murray, S.T., **Higgins, J.A.**, **Holmden, C.**, **Lu, C.** and **Swart, P.K.** (2021) Geochemical fingerprints of dolomitization in Bahamian carbonates: evidence from sulphur, calcium, magnesium, and clumped isotopes. *Sedimentology*, **68**, 1–29.

Murray, S.T. and **Swart, P.K.** (2017) Evaluating formation fluid models and calibrations using clumped isotope paleothermometry on Bahamian dolomites. *Geochim. Cosmochim. Acta*, **206**, 73–93.

Mylroie, J.E. and **Carew, J.L.** (1990) The flank margin model for dissolution cave development in carbonate platforms. *Earth Surf. Process. Landforms*, **15**, 413–424.

Nadeau, M., **Kimmig, S.R.** and **Holmden, C.** (2019) Basin-wide gradients in dolomite δ^{26}Mg and ^{87}Sr/^{86}Sr identify the structural centre of the Williston Basin as a source of magnesium for dolomitization of the Middle Devonian Winnipegosis Formation. In *Summary of Investigations 2019, Volume 1, Saskatchewan Geological Survey, Saskatchewan Ministry of Energy and Resources, Miscellaneous Report 2019–4.1, Paper A-1*, 21 p.

Nielsen, P., **Swennen, R.** and **Keppens, E.** (1994) Multiple-step recrystallization within massive ancient dolomite units: an example from the Dinantian of Belgium. *Sedimentology*, **41**, 567–584.

Nordeng, S.H. and **Sibley, D.F.** (1994) Dolomite stoichiometry and Ostwald's Step Rule. *Geochim. Cosmochim. Acta*, **58**, 191–196.

Onac, B., **Fornós, J.**, **Merino, A.**, **Ginés, J.** and **Diehl, J.** (2014) Linking mineral deposits to speleogenetic processes in Cova des Pas de Vallgornera (Mallorca, Spain). *Int. J. Speleol.*, **43**, 143–157.

Petrash, D.A., **Bialik, O.M.**, **Bontognali, T.R.R.**, **Vasconcelos, C.**, **Roberts, J.A.**, **McKenzie, J.A.** and **Konhauser, K.O.** (2017) Microbially catalyzed dolomite formation: From near-surface to burial. *Earth-Science Rev.*, **171**, 558–582.

Petrash, D.A., **Gueneli, N.**, **Brocks, J.J.**, **Mendez-Dot, J.A.**, **Gonzalez-Arismendi, G.**, **Poulton, S.W.** and **Konhauser, K.O.** (2016a) Black shale deposition and early diagenetic dolomite cementation during Oceanic Anoxic Event 1: The mid-Cretaceous Maracaibo Platform, northwestern South America. *Am. J. Sci.*, **316**, 669–711.

Petrash, D.A., **Lalonde, S.V.**, **González-Arismendi, G.**, **Gordon, R.A.**, **Méndez, J.A.**, **Gingras, M.K.** and **Konhauser, K.O.** (2015) Can Mn-S redox cycling drive sedimentary dolomite formation? A hypothesis. *Chem. Geol.*, **404**, 27–40.

Petrash, D.A., **Robbins, L.J.**, **Shapiro, R.S.**, **Mojzsis, S.J.** and **Konhauser, K.O.** (2016b) Chemical and textural overprinting of ancient stromatolites: Timing, processes, and implications for their use as paleoenvironmental proxies. *Precambrian Res.*, **278**, 145–160.

Plummer, L.N. (1975) Mixing of sea water with calcium carbonate ground water. In: *Quantitative Studies in the Geological Sciences* (Ed. Whitten, E.H.T.), *Memoir of the Geological Society of America*, **142**, 219–236.

Pohlman, J., **Iliffe, T.** and **Cifuentes, L.** (1997) A stable isotope study of organic cycling and the ecology of an anchialine cave ecosystem. *Mar. Ecol. Prog. Ser.*, **155**, 17–27.

Present, T.M., **Gutierrez, M.**, **Paris, G.**, **Kerans, C.**, **Grotzinger, J.P.** and **Adkins, J.F.** (2019) Diagenetic controls on the isotopic composition of carbonate-associated sulphate in the Permian Capitan Reef Complex, West Texas. *Sedimentology*, **66**, 2605–2626.

Present, T.M., **Paris, G.**, **Burke, A.**, **Fischer, W.W.** and **Adkins, J.F.** (2015) Large Carbonate Associated Sulfate isotopic variability between brachiopods, micrite, and other sedimentary components in Late Ordovician strata. *Earth Planet. Sci. Lett.*, **432**, 187–198.

Ren, M. and **Jones, B.** (2017) Spatial variations in the stoichiometry and geochemistry of Miocene dolomite from Grand Cayman: Implications for the origin of island dolostone. *Sediment. Geol.*, **348**, 69–93.

Ren, M. and **Jones, B.** (2018) Genesis of island dolostones. *Sedimentology*, **65**, 2003–2033.

Rennie, V.C.F. and **Turchyn, A.V.** (2014) The preservation of δSSO434 and δOSO418 in carbonate-associated sulfate during marine diagenesis: A 25 Myr test case using marine sediments. *Earth Planet. Sci. Lett.*, **395**, 13–23.

Riechelmann, S., **Mavromatis, V.**, **Buhl, D.**, **Dietzel, M.** and **Immenhauser, A.** (2020) Controls on formation and alteration of early diagenetic dolomite: A multi-proxy δ44/40Ca, δ26Mg, δ18O and δ13C approach. *Geochim. Cosmochim. Acta*, **283**, 167–183.

Riedinger, N., **Formolo, M.J.**, **Lyons, T.W.**, **Henkel, S.**, **Beck, A.** and **Kasten, S.** (2014) An inorganic geochemical argument for coupled anaerobic oxidation of methane and iron reduction in marine sediments. *Geobiology*, **12**, 172–181.

Rivers, J.M. and **Kaczmarek, S.E.** (2020) Dologrus: The impact of meteoric-water-controlled diagenesis following early-marine dolomitization. *Sedimentology*, **67**, 12742.

Roberts, J.A., **Kenward, P.A.**, **Fowle, D.A.**, **Goldstein, R.H.**, **González, L.A.** and **Moore, D.S.** (2013) Surface chemistry allows for abiotic precipitation of dolomite at low temperature. *Proc. Natl. Acad. Sci.*, **110**, 14540–14545.

Rodellas, V., **Garcia-Orellana, J.**, **Masqué, P.**, **Feldman, M.** and **Weinstein, Y.** (2015) Submarine groundwater discharge as a major source of nutrients to the Mediterranean Sea. *Proc. Natl. Acad. Sci.*, **112**, 3926–3930.

Rouxel, O., **Sholkovitz, E.**, **Charette, M.** and **Edwards, K.J.** (2008) Iron isotope fractionation in subterranean estuaries. *Geochim. Cosmochim. Acta*, **72**, 3413–3430.

Ryb, U. and **Eiler, J.M.** (2018) Oxygen isotope composition of the Phanerozoic ocean and a possible solution to the dolomite problem. *Proc. Natl. Acad. Sci. U. S. A.*, **115**, 6602–6607.

Sacks, L.A. and **Tihansky, A.B.** (1996) Geochemical and isotopic composition of ground water with emphasis on sources of sulfate in the upper Floridan Aquifer and intermediate aquifer system in southwest Florida. *U.S. Geolo. Survey, Water-Res Investig Rep*, **96–4146**, 54 pp.

Saller, A.H., **Budd, D.A.** and **Harris, P.M.** (1994) Unconformities and porosity development in carbonate strata: Ideas from a Hedberg Conference. *Am. Assoc. Pet. Geol. Bull.*, **79**, 857–872.

van Sambeek, M.H.G., **Eggenkamp, H.G.M.** and **Vissers, M.J.M.** (2000) The groundwater quality of Aruba, Bonaire and Curaçao: a hydrogeochemical study. *Netherlands. J. Geosci.*, **79**, 459–466.

Santoro, A.E. (2010) Microbial nitrogen cycling at the saltwater–freshwater interface. *Hydrogeol. J.*, **18**, 187–202.

Santos, I.R.S., **Burnett, W.C.**, **Chanton, J.**, **Mwashote, B.**, **Suryaputra, I.G.N.A.** and **Dittmar, T.** (2008) Nutrient biogeochemistry in a Gulf of Mexico subterranean estuary and groundwater-derived fluxes to the coastal ocean. *Limnol. Oceanogr.*, **53**, 705–718.

Santos, I.R., **Burnett, W.C.**, **Chanton, J.**, **Dimova, N.** and **Peterson, R.N.** (2009a) Land or ocean?: Assessing the driving forces of submarine groundwater discharge at a coastal site in the Gulf of Mexico. *J. Geophys. Res.*, **114**, C04012.

Santos, I.R., **Burnett, W.C.**, **Dittmar, T.**, **Suryaputra, I.G.N.A.** and **Chanton, J.** (2009b) Tidal pumping drives nutrient and dissolved organic matter dynamics in a Gulf of Mexico subterranean estuary. *Geochim. Cosmochim. Acta*, **73**, 1325–1339.

Santos, I.R., **Cook, P.L.M.**, **Rogers, L.**, **de Weys, J.** and **Eyre, B.D.** (2012) The "salt wedge pump": Convection-driven pore-water exchange as a source of dissolved organic and inorganic carbon and nitrogen to an estuary. *Limnol. Oceanogr.*, **57**, 1415–1426.

Scheller, S., **Yu, H.**, **Chadwick, G.L.**, **McGlynn, S.E.** and **Orphan, V.J.** (2016) Artificial electron acceptors decouple archaeal methane oxidation from sulfate reduction. *Science*, **351**, 703–707.

Searl, A. (1988) Mixing-zone dolomites in the Gully Oolite, Lower Carboniferous, south Wales. *J. Geol. Soc.*, **145**, 891–899.

Shatkay, M. and **Magaritz, M.** (1987) Dolomitization and sulfate reduction in the mixing zone between brine and meteoric water in the newly exposed shores of the Dead Sea. *Geochim. Cosmochim. Acta*, **51**, 1135–1141.

Sibley, D.F. (1980) Climatic Control of Dolomitization, Seroe Domi Formation (Pliocene), Bonaire, N.A. In: *Concepts and Models of Dolomitization* (Eds Zenger, D.H., Dunham, J.B. and Ethington, J.B.), *SEPM Special publication*, **28**, 247–258.

Sibley, D.F. (1982) The origin of common dolomite fabrics: Clues from the Pliocene. *J. Sediment. Res.*, **52**, 1087–1100.

Slaughter, M. and **Hill, R.J.** (1991) The influence of organic matter in organogenic dolomitization. *J. Sediment. Res.*, **61**, 296–303.

Śliwiński, M.G., **Kitajima, K.**, **Kozdon, R.**, **Spicuzza, M.J.**, **Fournelle, J.H.**, **Denny, A.** and **Valley, J.W.** (2016a) Secondary Ion Mass Spectrometry Bias on Isotope Ratios in Dolomite-Ankerite, Part I: δ^{18} O Matrix Effects. *Geostand. Geoanalytical Res.*, **40**, 157–172.

Śliwiński, M.G., **Kitajima, K.**, **Kozdon, R.**, **Spicuzza, M.J.**, **Fournelle, J.H.**, **Denny, A.** and **Valley, J.W.** (2016b) Secondary Ion Mass Spectrometry Bias on Isotope Ratios in Dolomite-Ankerite, Part II: δ^{13} C Matrix Effects. *Geostand. Geoanalytical Res.*, **40**, 173–184.

Smart, P.L., **Dawans, J.M.** and **Whitaker, F.** (1988) Carbonate dissolution in a modern mixing zone. *Nature*, **335**, 811–813.

Socki, R.A., **Perry, E.J.C.** and **Romanek, C.S.** (2002) Stable isotope systematics of two cenotes from the northern Yucatan Peninsula, Mexico. *Limnol. Oceanogr.*, **47**, 1808–1818.

Soetaert, K., **Hofmann, A.F.**, **Middelburg, J.J.**, **Meysman, F.J.R.** and **Greenwood, J.** (2007) The effect of biogeochemical processes on pH. *Mar. Chem.*, **105**, 30–51.

Sørensen, J. (1987) Nitrate reduction in marine sediment: Pathways and interactions with iron and sulfur cycling. *Geomicrobiol. J.*, **5**, 401–421.

Spratt, R.M. and **Lisiecki, L.E.** (2015) A Late Pleistocene sea level stack. *Clim. Past Discuss.*, **11**, 3699–3728.

Starke, R., **Müller, M.**, **Gaspar, M.**, **Marz, M.**, **Küsel, K.**, **Totsche, K.U.**, **von Bergen, M.** and **Jehmlich, N.** (2017) Candidate Brocadiales dominates C, N and S cycling in anoxic groundwater of a pristine limestone-fracture aquifer. *J. Proteomics*, **152**, 153–160.

Staudigel, P.T., **Higgins, J.A.** and **Swart, P.K.** (2021) An abrupt Middle-Miocene increase in fluid flow into the Leeward Margin Great Bahama Bank, constraints from δ44Ca and Δ47 values. *Earth Planet. Sci. Lett.*, **553**, 116625.

Stoessell, R.K. (1992) Effects of sulfate reduction on CaCO3 dissolution and precipitation in mixing-zone fluids. *J. Sediment. Petrol.*, **62**, 873–880.

Stoessell, R.K., **Ward, W.C.**, **Ford, B.H.** and **Schuffert, J.D.** (1989) Water chemistry and $CaCO_3$ dissolution in the saline part of an open-flow mixing zone, coastal Yucatan Peninsula, Mexico. *Geol. Soc. Am. Bull.*, **101**, 159–169.

Stüben, D., **Sedwick, P.** and **Colantoni, P.** (1996) Geochemistry of submarine warm springs in the limestone cavern of Grotta Azzurra, Capo Palinuro, Italy: Evidence for mixing-zone dolomitisation. *Chem. Geol.*, **131**, 113–125.

Sumrall, J.B., **Larson, E.B.** and **Mylroie, J.E.** (2016) Dolomite caves within the Seroe Domi Formation on Curacao, Netherland Antilles. *Acta Carsologica*, **45**, 19–32.

Sumrall, J., **Mylroie, J.** and **Kambesis, P.** (2015) Microbial mixing zone dolomitization and karst development within Isla de Mona Dolomite, Isla de Mona, Puerto Rico. *Carbonate Evaporite*, **30**, 45–58.

Swart, P.K. and **Melim, L.A.** (2000) The Origin of Dolomites in Tertiary Sediments from the Margin of Great Bahama Bank. *J. Sediment. Res.*, **70**, 738–748.

Swart, P.K. and **Oehlert, A.M.** (2018) Revised interpretations of stable C and O patterns in carbonate rocks resulting from meteoric diagenesis. *Sediment. Geol.*, **364**, 14–23.

Taberner, C. and **Santisteban, C.** (1987) Mixed-water dolomitization in a transgressive beach-ridge system, Eocene Catalan Basin, NE Spain. *Geol. Soc. Spec. Publ.*, **36**, 123–139.

Tang, J. and **Johannesson, K.H.** (2005) Rare earth elements in groundwater flow systems In: *Rare Earth Elements in Groundwater Flow Systems* (Ed. Johannesson, K.H.), pp. 223–251. Springer, Berlin.

Taniguchi, M. (2002) Tidal effects on submarine groundwater discharge into the ocean. *Geophys. Res. Lett.*, **29**, 1561.

Teal, C.S., **Mazzullo, S.J.** and **Bischoff, W.D.** (2000) Dolomitization of Holocene shallow-marine deposits mediated by sulfate reduction and methanogenesis in normal-salinity seawater, Northern Belize. *J. Sediment. Res.*, **70**, 649–663.

Thiel, V. (2018) Methane carbon cycling in the past: Insights from hydrocarbon and lipid biomarkers. In: *Hydrocarbons, Oils and Lipids: Diversity, Origin, Chemistry and Fate* (Eds Wilkes, H. and Volker, T.), pp. 1–30.Springer International Publishing, Cham.

Thorstenson, D.C. and **Mackenzie, F.T.** (1974) Time variability of pore water chemistry in recent carbonate sediments, Devil's Hole, Harrington Sound, Bermuda. *Geochim. Cosmochim. Acta*, **38**, 1–19.

Vahrenkamp, V.C. and **Swart, P.K.** (1990) New distribution coefficient for the incorporation of strontium into dolomite and its implications for the formation of ancient dolomites. *Geology*, **18**, 387.

Vahrenkamp, V. and **Swart, P.** (1994) Late Cenozoic dolomites of the Bahamas: metastable analogues for the genesis of ancient platform dolomites. In: *Dolomites: A Volume in Honour of Dolomieu* (Eds Purser, B.H., Tucker, M.E. and Zenger, D.H.), pp. 133–153. John Wiley & Sons, New York, NY.

Van Lith, Y., **Warthmann, R.**, **Vasconcelos, C.** and **Mckenzie, J.A.** (2003) Sulphate-reducing bacteria induce low-temperature Ca-dolomite and high Mg-calcite formation. *Geobiology*, **1**, 71–79.

Vandeginste, V., **Snell, O.**, **Hall, M.R.**, **Steer, E.** and **Vandeginste, A.** (2019) Acceleration of dolomitization by zinc in saline waters. *Nat. Commun.*, **10**, 1851.

Vasconcelos, C., **McKenzie, J.A.**, **Bernasconi, S.**, **Grujic, D.** and **Tiens, A.J.** (1995) Microbial mediation as a possible mechanism for natural dolomite formation at low temperatures. *Nature*, **377**, 220–222.

Ward, W.C. and **Halley, R.B.** (1985) Dolomitization in a mixing zone of near-seawater composition, Late Pleistocene, Northeastern Yucatan Peninsula. *J. Sediment. Res.*, **55**, 407–420.

Warthmann, R., **van Lith, Y.**, **Vasconcelos, C.**, **McKenzie, J.A.** and **Karpoff, A.M.** (2000) Bacterially induced dolomite precipitation in anoxic culture experiments. *Geology*, **28**, 1091.

Westerhold, T., **Marwan, N.**, **Drury, A.J.**, **Liebrand, D.**, **Agnini, C.**, **Anagnostou, E.**, **Barnet, J.S.K.**, **Bohaty, S.M.**, **De Vleeschouwer, D.**, **Florindo, F.**, **Frederichs, T.**, **Hodell, D.A.**, **Holbourn, A.E.**, **Kroon, D.**, **Lauretano, V.**, **Littler, K.**, **Lourens, L.J.**, **Lyle, M.**, **Pälike, H.**, **Röhl, U.**, **Tian, J.**, **Wilkens, R.H.**, **Wilson, P.A.** and **Zachos, J.C.** (2020) An astronomically dated record of Earth's climate and its predictability over the last 66 million years. *Science*, **369**, 1383–1387.

Whitaker, F.F. and **Smart, P.S.** (1998) Hydrology, geochemistry and diagenesis of fracture blue holes, South Andros, Bahamas. *Cave Karst Sci.*, **25**, 75–82.

Whitaker, F.F., **Smart, P.L.**, **Vahrenkamp, V.C.**, **Nicholson, H.** and **Wogelius, R.A.** (1994) Dolomitization by near-normal seawater? Field evidence from the Bahamas. In: *Dolomites: A Volume in Honour of Dolomieu* (Eds Purser, B.H., Tucker, M.E. and Zenger, D.H.), *IAS Spec. Publ.*, **21**, pp. 111–132. Blackell Scientific, Oxford.

Wicks, C.M., **Herman, J.S.**, **Randazzo, A.F.** and **Jee, J.L.** (1995) Water-rock interactions in a modern coastal mixing zone. *Geol. Soc. Am. Bull.*, **107**, 1023–1032.

Wigley, T.M.L. and **Plummer, L.N.** (1976) Mixing of carbonate waters. *Geochim. Cosmochim. Acta*, **40**, 989–995.

Winkelstern, I.Z. and **Lohmann, K.C.** (2016) Shallow burial alteration of dolomite and limestone clumped isotope geochemistry. *Geology*, **44**, 467–470.

Wolf-Gladrow, D.A., **Zeebe, R.E.**, **Klaas, C.**, **Körtzinger, A.** and **Dickson, A.G.** (2007) Total alkalinity: The explicit conservative expression and its application to biogeochemical processes. *Mar. Chem.*, **106**, 287–300.

Wright, D.T. and **Wacey, D.** (2005) Precipitation of dolomite using sulphate-reducing bacteria from the Coorong Region, South Australia: Significance and implications. *Sedimentology*, **52**, 987–1008.

Wurgaft, E., **Findlay, A.J.**, **Vigderovich, H.**, **Herut, B.** and **Sivan, O.** (2019) Sulfate reduction rates in the sediments of the Mediterranean continental shelf inferred from combined dissolved inorganic carbon and total alkalinity profiles. *Mar. Chem.*, **211**, 64–74.

Xiao, Y., **Jones, G.D.**, **Whitaker, F.F.**, **Al-Helal, B.**, **Stafford, S.**, **Gomez-Rivas, E.** and **Guidry, S.** (2013) Fundamental approaches to dolomitisation and carbonate diagenesis in different hydrogeological systems and the impact on reservoir quality distribution In: *International Petroleum Technology Conference 2013, IPTC 2013: Challenging Technology and Economic Limits to Meet the Global Energy Demand, International Petroleum Technology Conference*, **2**, 1164–1179.

Xun, Z. and **Fairchild, I.J.** (1987) Mixing zone dolomitization of Devonian carbonates, Guangxi, South China. *Geol. Soc. Spec. Publ.*, **36**, 157–170.

Zeebe, R.E. and **Wolf-Gladrow, D.** (2001) *CO_2 in Seawater: Equilibrium, Kinetics, Isotopes*. Elsevier, Amsterdam, 360 pp.

Zhang, F., **Xu, H.**, **Konishi, H.**, **Kemp, J.M.**, **Roden, E.E.** and **Shen, Z.** (2012a) Dissolved sulfide-catalyzed precipitation of disordered dolomite: Implications for the formation mechanism of sedimentary dolomite. *Geochim. Cosmochim. Acta*, **97**, 148–165.

Zhang, F., **Xu, H.**, **Konishi, H.**, **Shelobolina, E.S.** and **Roden, E.E.** (2012b) Polysaccharide-catalyzed nucleation and growth of disordered dolomite: A potential precursor of sedimentary dolomite. *Am. Mineral.*, **97**, 556–567.

Zhao, H. and **Jones, B.** (2012) Origin of "island dolostones": A case study from the Cayman Formation (Miocene), Cayman Brac, British West Indies. *Sediment. Geol.*, **243–244**, 191–206.

Zhao, M., **Planavsky, N.**, **Oehlert, A.M.**, **Wei, G.** and **Gong, Z.** (2020) Simulating meteoric and mixing zone carbonate diagenesis with a two-dimensional reactive transport model. *Am. J. Sci.*, **320**, 599–636.

Zuddas, P. and **Mucci, A.** (1994) Kinetics of calcite precipitation from seawater: I. A classical chemical kinetics description for strong electrolyte solutions. *Geochim. Cosmochim. Acta*, **58**, 4353–4362.

Manuscript received 12 February 2020; revision accepted 26 January 2021